Indian Geotech J
https://doi.org/10.1007/s40098-023-00765-w

ORIGINAL PAPER

Instrumentation and Data Interpretation in Transportation Geotechnics

Buddhima Indraratna[1] · Rakesh Sai Malisetty[1] · Lakshmi Nair[1] · Cholachat Rujikiatkamjorn[1]

Received: 31 January 2023 / Accepted: 28 July 2023

Abstract Transportation networks on the eastern coast of Australia are often built on or traverse coastal flood plains and marine clays with unfavourable soil conditions. In the past two decades, a significant number of laboratory investigations were carried out in soft soil improvement using Prefabricated Vertical Drains (PVDs) combined with vacuum-assisted surcharge preloading. In addition, significant research efforts were made to reduce the maintenance costs of railway tracks and increase their longevity by using synthetic inclusions such as geocomposites, geogrids and shock mats. These research outcomes were implemented and validated in practice through several field investigations along the eastern coast of Australia. This paper demonstrates the significance of instrumentation and data interpretation in geotechnical field investigations through 6 case histories. Field trials including Port of Brisbane Land Reclamation, Ballina Bypass Upgrade and Sandgate Rail Separation Projects were presented highlighting innovative ways of monitoring the performance of PVDs with vacuum and non-vacuum surcharge preloading. Also, railway track design improvements using geosynthetic and shock mats were discussed through Bulli and Singleton trial track case studies. Further, the heavy haul track testing facility at Russell Vale, New South Wales, was discussed as an alternative for expensive and time-consuming field trials.

Keywords Prefabricated vertical drains · Instrumentation · Ballasted railway tracks · Vacuum preloading

✉ Buddhima Indraratna
Buddhima.indraratna@uts.edu.au

[1] Transport Research Centre, University of Technology Sydney, Ultimo, NSW 2007, Australia

Introduction

The rapid population growth along the eastern coast of Australia has increased the need for transportation infrastructure. Much of the east coast of Australia is underlain by soft alluvial clays which possess low undrained shear strength and high compressibility [1]. Construction of different types of transportation infrastructures such as rail and road networks, commercial ports, etc., on such soils, poses a significant challenge to geotechnical engineers to build safer and more stable infrastructure. Road and railway networks play a crucial role in the economy through the transportation of freight and bulk commodities from commercial ports to major cities and regional centres in the country. Building infrastructure on soft marine and alluvial soils can lead to excessive surface settlements as well as the generation of excess pore water pressures. In railway tracks, these excess pore-water pressures if not dissipated quickly can pump up into the ballast layer, severely affecting the drainage capacity and causing track instability [2, 3]. Therefore, it is imperative to apply different ground improvement techniques to the existing soft soils to prevent unacceptable settlements, and lateral movements and provide stability to foundations. Some of these ground improvement techniques include Prefabricated Vertical Drains (PVDs) and surcharge preloading for quicker and more effective consolidation [4–9]. A combination of PVDs with surcharge using vacuum preloading instead of traditional preloading was proved to accelerate the consolidation process. In addition, through the application of vacuum pressure, the surcharge height can be reduced while keeping the same total pressure. These types of ground improvement techniques demonstrate their usefulness while building commercial ports on reclaimed land such as Port of Brisbane and road highway embankments at Ballina on soft alluvial soils [7, 10, 11]. In addition, PVDs are also found to

Published online: 15 August 2023

be efficient in dissipating excess pore water pressures generated by cyclic loads from moving trains [5].

In addition to the problems associated with soft subgrade soils, a significant portion of the railway maintenance budget in Australia is related to ballast problems such as ballast degradation and ballast fouling, both from broken ballast particles and pumped-up clay from subgrades [12–14]. Routine maintenance procedures involve the replacement of fouled ballast with fresh ballast and have resulted in vast stockpiles of waste ballast. Ballast disposal has not only become an ongoing problem for railway asset owners to comply with the Environment Protection Authority (EPA) but also demands additional quarrying depleting limited resources [15]. In recent times, there have been significant efforts made for understanding the working principles of ballasted railway tracks. Upon prolonged cycles of train loading, ballast aggregates degrade resulting in the adverse consequences of ballast fouling, reduced drainage capacity, and reduction in the ultimate bearing capacity of the track [16–18]. Several laboratory studies conducted on the use of polymeric geosynthetics (geocells, geogrids, geotextiles and geocomposites), and rubber mats in traditional track design reported an increase in the bearing capacity of railway tracks as well as reducing the degradation of ballast aggregates [12, 14, 15, 19–22]. Polymeric geogrids are widely used to reinforce the ballast layer and by using an appropriate aperture size, this technique is proven to increase ballast shear strength by increasing interlock and reduce particle degradation by restricting lateral movements of ballast [23]. To minimise the effects of impact loads caused by wheel irregularities such as wheel flats, rail squats, etc., Under Ballast Mats (UBM) made of rubber can be used at the ballast-concrete interface on bridge decks that can attenuate the dynamic forces in the ballast layer and can reduce ballast degradation [22, 24]. In addition, they are also efficient in reducing vertical deformations by 10–20% and lateral displacements by 5–10% [22]. Jayasuriya et. al. [25] investigated the use of another form of shock mats placed underneath the sleeper (Under Sleeper Pads, USP) and reported that the effective sleeper-ballast contact area was increased by USPs which resulted in minimising the stress concentration onto ballast aggregates. Embracing circular economy principles, the utilisation of recycled waste tyres in different forms (tyre with the side wall removed, rubber crumbs, chips, etc.) in rail substructure layers was investigated in recent years [26, 27]. The enhanced damping capacity of rubber elements will aid in reducing the dilatancy of ballast and increases the energy absorption capacity of the overall track. Laboratory testing on a capping layer reinforced with passenger car tyres with the side wall removed proved an increase in track stiffness by more than 50% [28]. While laboratory testing and analysis provides an overview of the mechanical behaviour of different soils in a controlled and confined environment, it is common to use idealised conditions such as loading parameters, material state, boundary and scale effects, etc., which differ from field situations. As much as investigating the fundamental concepts in the laboratory, it is important to verify the research innovations in practice to validate their economic feasibility and workability.

Role of Instrumentation in Transportation Geotechnics

Geotechnical field investigations related to transportation infrastructure often involve complex geological conditions in which the soil properties vary spatially with distance and with time. Due to the limited equipment dimensions, laboratory testing cannot mimic the exact field performance. For example, large-scale triaxial tests on ballast provide accurate information about the influence of confining stress, loading frequency, and amplitude on the ballast deformations; however, they cannot capture the effects of moving loads and resting periods between consecutive train passages. In such cases, field instrumentation and data collection play an essential role in accurately investigating the spatial variation of geological conditions, climate variations, and degradation of geotechnical structures pertaining to the performance of different research innovations [29]. It is important to understand the difference in the instrumentation process between laboratory and field and the use of sophisticated data acquisition systems to record and store the data recordings in harsh environments. In addition, data obtained from a fully instrumented field trial is crucial for accurately estimating the benefits of different ground improvement techniques and data interpretation plays a key role while analysing the outcomes.

While it is essential to conduct in situ tests to understand the soil/rock properties during the design phase such as shear strength, compressibility, permeability, etc., it is equally important to monitor the ongoing infrastructure's performance. Different instruments are used for monitoring the performance of an infrastructure [10, 30]. These instruments can be grouped into two categories. The first category includes instruments that need manual inspections, and the second category includes instruments and sensors that are equipped with automatic monitoring technologies. Use of remote sensing instruments such as displacement monitoring cameras using advanced digital image correlation algorithms have also been used to measure rail and sleeper movements, defects in rail components, etc. [31, 32]. In addition, accelerometers fitted onboard in-service trains are recently explored to monitor the condition of the track based on intelligent systems [33, 34]. An integrated data acquisition system with these intelligent instruments will provide valuable insights into the current condition of the infrastructure that can be

used to inform maintenance decisions. In addition, they are useful to determine parameters such as load cycles, train speeds, surcharge loads, etc., which are essential to transport management. However, the accuracy of intelligent systems often depends on rigorous training through large databases and requires the correlation of sensor readings with track substructure problem history. A few selected instruments that are typically used in transportation infrastructure are shown in Table 1.

Through several years of research, several instruments were used in field investigations applying the research innovations through separate case studies along the eastern coast of Australia as shown in Fig. 1. PVDs were used in the projects of Port of Brisbane, Sandgate rail upgrade and Ballina trial embankment, where the consolidation process was carefully monitored through the different phases of the project [6, 19, 35]. Innovations related to railway infrastructure were implemented in sections of instrumented rail tracks at Singleton and Bulli, New South Wales, Australia with the support of the Australian Rail Track Corporation and Transport for New South Wales (previously Sydney Trains), respectively [20, 21]. Further, a full-scale track testing facility at Russell Vale, New South Wales, Australia was used to demonstrate the use of recycled rubber tyres in enhancing the stability of ballasted railway track. The details of instruments used and how they helped to monitor the performance of different transportation infrastructure is detailed in the following case studies. This paper also emphasises data interpretation of these six full-scale field trials to validate the effectiveness of research innovations applied in practice.

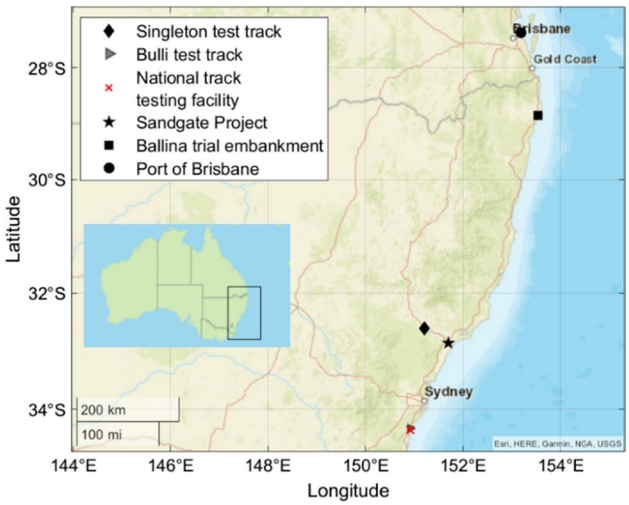

Fig. 1 Field studies on transport networks along the eastern coast of Australia

Land Reclamation at Port of Brisbane

Port of Brisbane was one of the large container shipping ports on the east coast of Australia at Fisherman Island near the mouth of the Brisbane River. To handle the increasing demand for trading activities at the port, a new area of about 235 hectares was reclaimed and improved in 2010 as an extension to the Port of Brisbane (Fig. 2). The soil in this area was highly compressible and of low shear strength. Ground improvement using PVDs was initially proposed to facilitate the consolidation process, and a combination of surcharge with vacuum preloading was trialled to accelerate the consolidation. The current case study's scope includes comparing Prefabricated Vertical Drains with vacuum and non-vacuum (with surcharge load) systems. A trial area named S3A is considered for the current study.

Trial Embankment Characteristics

The S3A area proposed for reclamation was divided into the vacuum (VC1-VC2) and non-vacuum areas (WD1-WD5), as shown in Fig. 3. The soil profile of the site consisted of

Table 1 Field instruments used in transportation infrastructure

Objectives	Instrument types	Intended placement
Settlement measurement	Settlement pegs/probes	Sleeper, ballast, subgrade
Lateral displacements/deformations measurement	Extensometers, inclinometers linear variable differential transducers (LVDT)	Ballast, subgrade
In situ stress measurement	Pressure cells	Rails, sleepers, ballast, subgrade
Vibration measurement	Accelerometers, geophones	Rails, sleepers, embankment surface
Surface deflection measurement	Motion sensing cameras	Rails, sleepers
Pore-pressure measurement	Vibrating wire piezometers, standpipe piezometers, pore pressure transducers	Subgrade/embankment
Soil moisture measurement	Moisture sensors (ADR—Amplitude domain reflectometry)	Subgrade/embankment
Soil matric suction measurement	Tensiometers	Subgrade/embankment
Directional strain measurement	Multi-axial strain gauges	Rails, artificial inclusions (geogrids, shock mats, etc.)

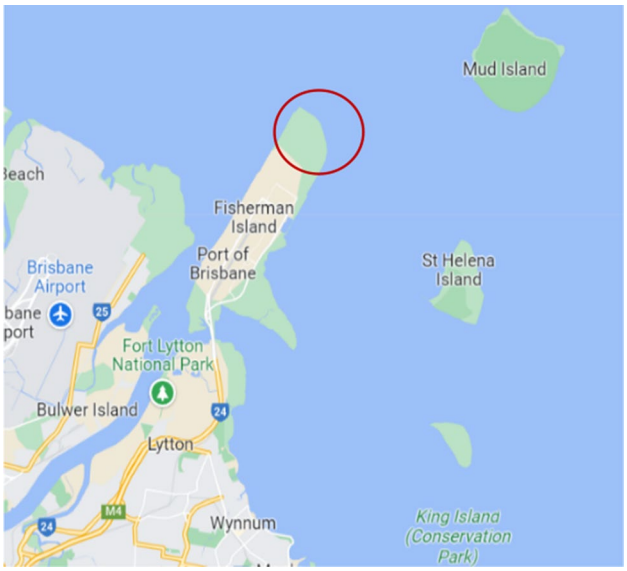

Fig. 2 Map of the extended area (encircled) at Port of Brisbane (source: Google Maps)

an upper Holocene sand layer of about 2-3 m thick overlying a Holocene clay deposit of 6–25 m thick, followed by a highly over consolidated Pleistocene clay [36]. A sand layer was laid on top of upper Holocene sand for the installation of PVD and to provide a drainage layer for vacuum systems. The ground improvement technique adopted in the site includes preloading with surcharge and membrane vacuum consolidation system with PVDs. The design specification included a maximum residual settlement of not exceeding 250 mm over 20 years of 15–25 kPa service load application. Table 2 details the PVD, embankment height and treatment method used in different sub-divisions of area S3A. Different drain lengths were used due to different clay thicknesses.

Circular drains of diameter 34 mm at a spacing of 1.2 m were installed in sections VC1 and VC2. The membrane-type vacuum preloading was adopted in these sections. After installing the PVDs, the sand blanket was placed with horizontal perforated pipes. Subsequently, a membrane was laid on top with its end submerged in a bentonite slurry trench. This trench is a deep cut-off wall (of 15 m depth) provided along the periphery of the trial area and filled with soil-bentonite slurry to ensure air tightness during the vacuum application [7, 36]. The instrumentations included vibrating wire piezometers, settlement plates magnetic extensometers and inclinometers. The inclinometers were installed at various depths from the sand platform in different areas ranging from 5-18 m.

Field Instrumentation and Observations

The data from field instruments were analysed in detail to compare the performance of vacuum and non-vacuum systems of consolidation. Settlement plates, vibrating wire piezometers, magnetic extensometers and inclinometers were used to obtain the settlement, pore pressure and lateral displacements, respectively. The embankment

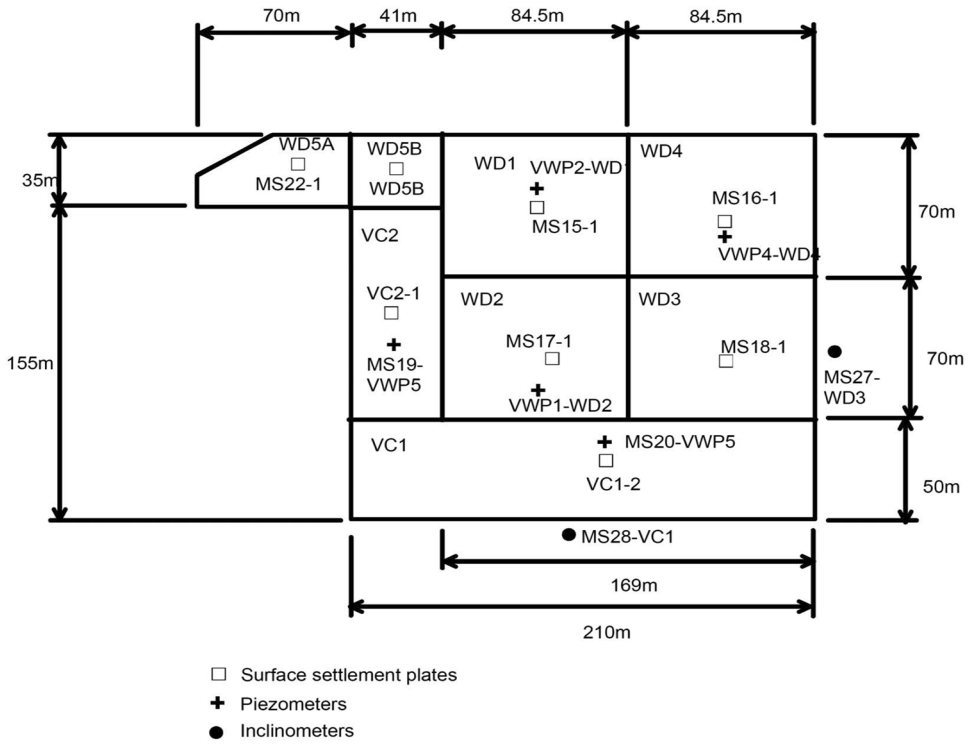

Fig. 3 Sub-divisions and instrument layout (plan view) of S3A area (sourced from Indraratna et al.[36])

Table 2 PVD characteristics and treatment methods for different sections [36]

Section	Drain type	Drain length (m)	Drain spacing (m)	Clay thickness (m)	Total fill height (m)	Treatment method
WD1	Circular drains-34 mm diameter	14.5–18.5	1.1	12.0–15.5	5.2	Surcharge
WD2	Circular drains-34 mm diameter	22.5–27.5	1.3	20.0–23.5	7–7.2	Surcharge
WD3	Band drain Type –A (100 × 4 mm^2)	17.1–23.5	1.1	14.0–17.0	4.3–4.6	Surcharge
WD4	Band drain Type –A (100 × 4 mm^2)	27.0–28.7	1.3	22.5–24.5	6.1	Surcharge
WD5A	Band drain Type –B (100 × 4 mm^2)	6.0–8.0	1.2	6.0–8.0	3.3	Surcharge
WD5B	Band drain Type –B (100 × 4 mm^2)	13.5	1.1	9.5	5.5	Surcharge
VC1	Circular drains-34 mm diameter	14.0–26.5	1.2	9.0–21.0	3.2	Surcharge + 70 kPa vacuum
VC2	Circular drains-34 mm diameter	15.5–22.5	1.2	12.5–18.5	2.8	Surcharge + 70 kPa vacuum

response in the form of settlements and pore pressure was plotted along with the stage embankment construction in Fig. 4. The embankment heights are different depending on the thickness of the clay layer for each section, as seen in Table 3. Figure 4 shows that the initial settlement trend is similar. However, the ultimate settlement depends on the clay layer thickness and embankment height, with the highest settlement occurring for WD4 (clay layer of 19–26 m thick) and the lowest settlement for WD5A.

The strain-based DOC of different areas is shown in Table 3. When considering sections with similar clay thickness, the DOC of VC2 is significantly higher than that of WD2. Furthermore, the vacuum application also helps reduce the cost of surcharge removal, as is evident from the fill height required for two locations.

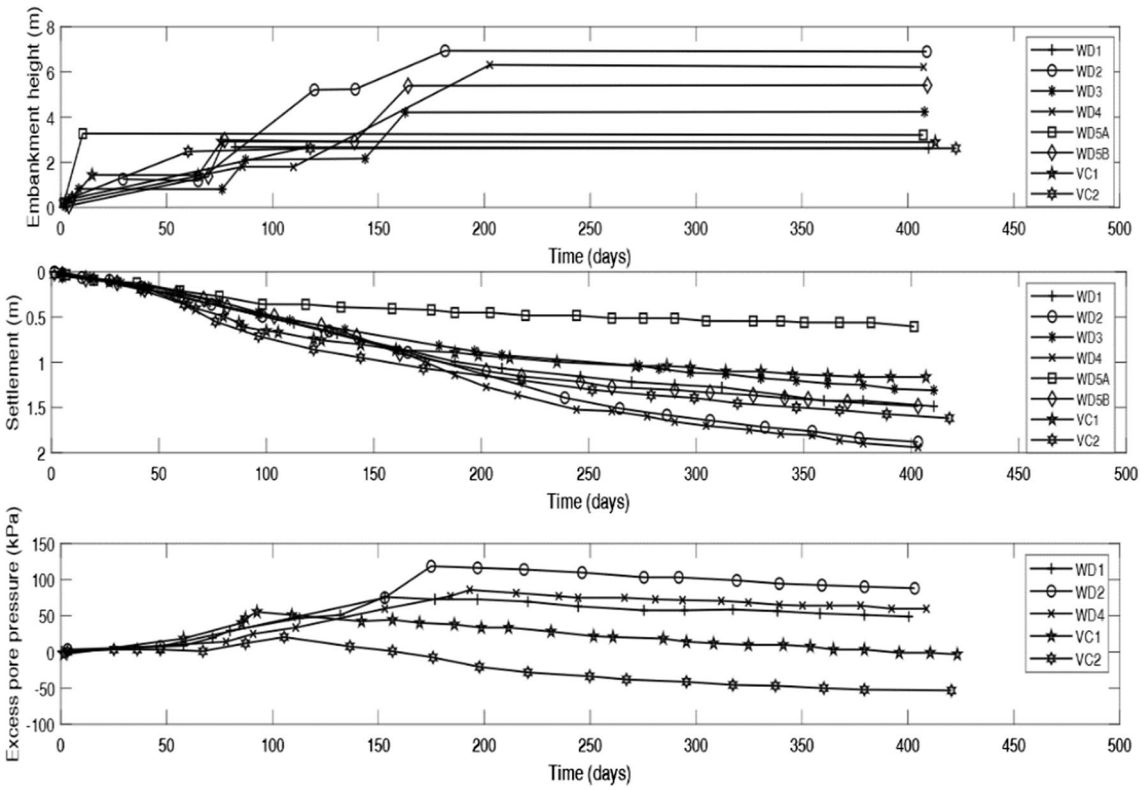

Fig. 4 Embankment height, settlement and excess pore pressure at different sub-sections of S3A (data sourced from Indraratna et. al. [36])

Table 3 Clay Layer thickness, embankment height and Degree of Consolidation (after 400 days) for different sub-divisions of the S3A section [36]

Sub-divisions of section S3A	Upper holocene clay layer thickness (m)	Lower holocene clay layer thickness (m)	Degree of consolidation (DOC) after 400 days (strain-based)
WD1 (Surcharge only)	4–6	10–12	92
WD2 (Surcharge only)	2–5	18–20	82
WD3 (Surcharge only)	2–3	8–15	87
WD4 (Surcharge only)	1.5–3.5	18–23	85
WD5A (Surcharge only)	2–4	6–8	94
WD5B (Surcharge only)	2–4	7–8	92
VC1 (Surcharge plus 70 kPa vacuum)	2–3	5–18	87
VC2 (Surcharge plus 70 kPa vacuum)	2–3	9–16	90

The pore pressure reduction with time was compared for different areas to compare the performance of conventional surcharge and vacuum systems of preloading. Figure 4 shows that the regions subjected to vacuum preloading exhibit higher pore pressure dissipation, which highlights the effectiveness of vacuum consolidation in discharging pore pressure. It is to be noted that the negative excess pore pressures were observed for VC1 and VC2 due to the effect of vacuum application at the site. The negative pore pressure approached the applied vacuum pressure (~ 70 kPa) with time for the case of VC1 and VC2. However, there is a mismatch which was observed between degrees of consolidation obtained from settlement (strain based) and excess pore pressure trend after 200 days and this is not uncommon for the field measurement applicable soil consolidation induced by radial drainage. Indraratna et al. [6] show that the rate of excess pore water pressure dissipation is much slower compared to the rate of settlement. This can be attributed to the effect of clay viscosity and the clogging of the piezometer tips. Lateral movement in the vacuum and the non-vacuum area was compared using the inclinometers' data for sections VC1 and WD3. Figure 5 shows the measured lateral displacement normalized with the total change in applied stresses at surface settlement plates MS28 (vacuum area VC1) and MS27 (non-vacuum area WD3). In the WD3 area, the total surcharge pressure was 90 kPa, corresponding to a surcharge height of 4–5 m, and in the VC1 area, a 2 m surcharge height (40 kPa) was applied in addition to 65 kPa vacuum pressure. From Fig. 5, it is evident that consolidation with vacuum pressure helps in curtailing lateral movement. The ratio of maximum horizontal displacement to vertical settlement (μ) was considered a stability indicator and plotted along with time. The ratio for the area VC1 was lower than the area WD3, as shown in Fig. 6, indicating the vacuum's effectiveness in reducing lateral displacements.

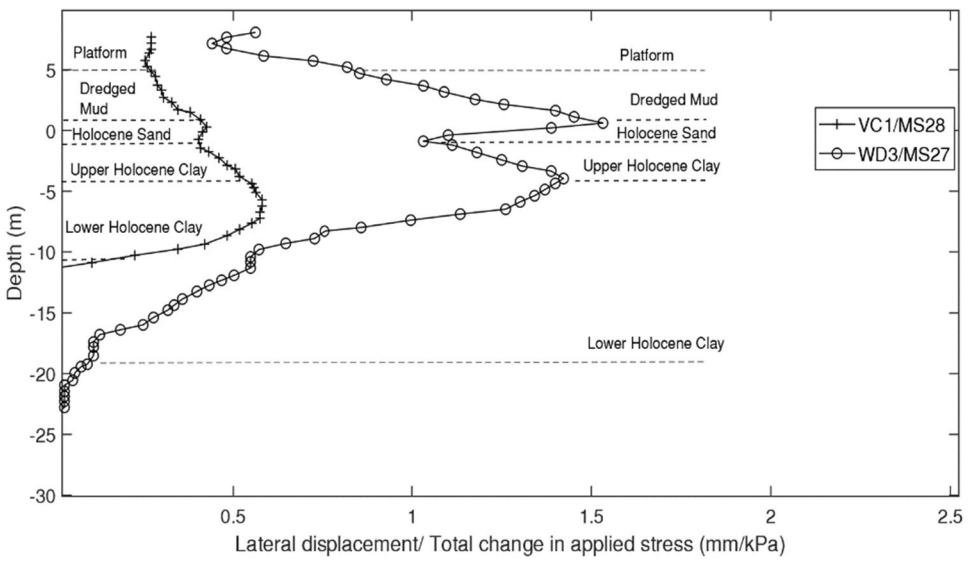

Fig. 5 Ratio of lateral displacement to total change in applied stress compared for vacuum and non-vacuum areas after 400 days (data sourced from Indraratna et. al. [36])

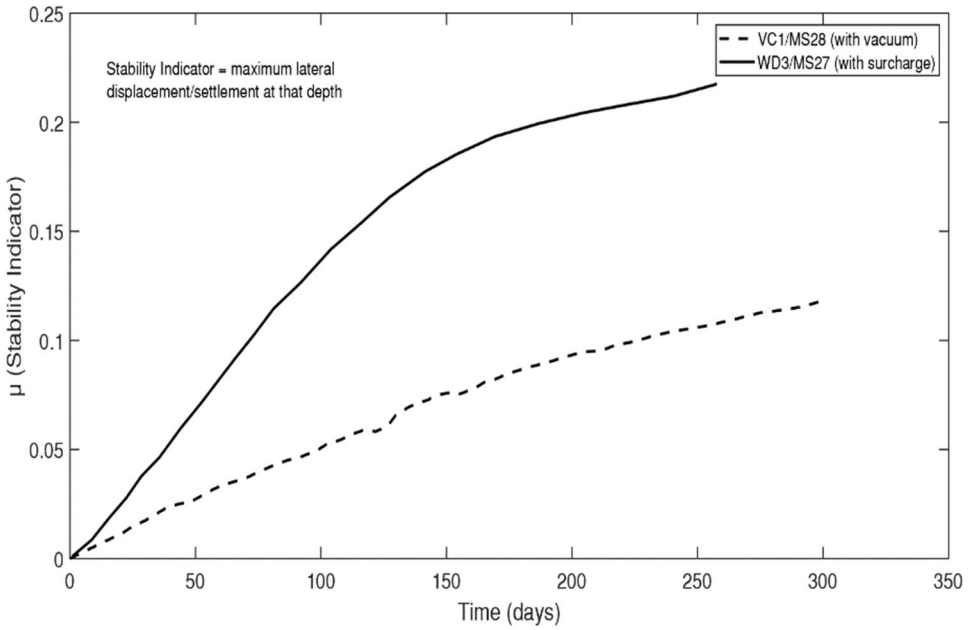

Fig. 6 Stability indicator (lateral displacement/surface settlement) at the location of MS27 and MS28 plotted with time (data sourced from Indraratna et. al. [36])

Table 4 In situ properties of the soft and medium silty clay layer (data from Indraratna et al. [11])

Properties	Values
Water content	80–120%
Shear strength	5–40 kPa
Compression Index	0.30–0.50

Ballina Trial Embankment

Vacuum-assisted surcharge loading with PVDs (with membrane) was also used at Ballina, NSW, to stabilise road embankments and improve the deep estuarine deposits by reducing the time required for consolidation. As a part of the Pacific Highway upgrade, a bypass route was planned to support the high traffic demands between Australia's northern and eastern coastal belts, linking Sydney and Brisbane. The route was designed to pass over a low-lying floodplain with highly compressible marine clay up to 30 m depth. In situ observations show that the soil profile consists of approximately 2–2.7 m thick alluvium soft soil as the top layer, underlain by very soft clay of 12 m thickness [37]. The soft clay deposit is followed by a 15 m thick, firm silty clay layer. The groundwater level at the site fluctuates between 0.5 and 1 m below the ground surface. It is mainly elevated due to seepage after heavy rainfall or tidal influx. The in situ properties of the soil are listed in Table 4.

The effectiveness of the proposed ground improvement technique was tested using a trial embankment at the southern approach to Emigrant Creek, which is to the north of Ballina. A total area of approximately 9500 m^2 was installed with 34 mm diameter circular drains in a square pattern at a spacing of 1.0 m. For the area on which vacuum pressure was applied, an impervious membrane was laid on the sand blanket overlying the PVDs installed. The membrane edges were submerged in the peripheral bentonite slurry trench to maintain air tightness, and heavy-duty vacuum pumps with horizontal transmission pipes were provided for the uniform distribution of vacuum pressure [11].

Field instruments including surface settlement plates, inclinometers and piezometers were installed on the site. Figure 7 shows the location of field instrumentation at the test embankments. The piezometers were placed at 1.3, 4.5, and 8 m below the ground surface, and eight inclinometers were installed at the embankment edges.

Data Interpretation

The construction of the embankment was completed in stages. The embankment sections without and with vacuum are named section A and B, respectively. During the initial 100 days, the embankment was raised to 4–8 m. After 90 days, vacuum suction in the range of 70–80 kPa was applied for 200 days. The second stage of embankment construction commenced after 660 days, and the surcharge preloading ceased after 1200 days.

Figure 8 shows the staged embankment construction along with the settlement and excess pore pressure data. The data from selected settlement plates SP1, SP3, SP5, SP7, SP9 and SP11 show that after 1200 days, the vertical strains range between 14 and 24%. The difference in clay depth and thickness (as shown in Table 5) result in significant variations in time-settlement curves. The vertical strain is lowest in the non-vacuum area (SP1) because of the smaller

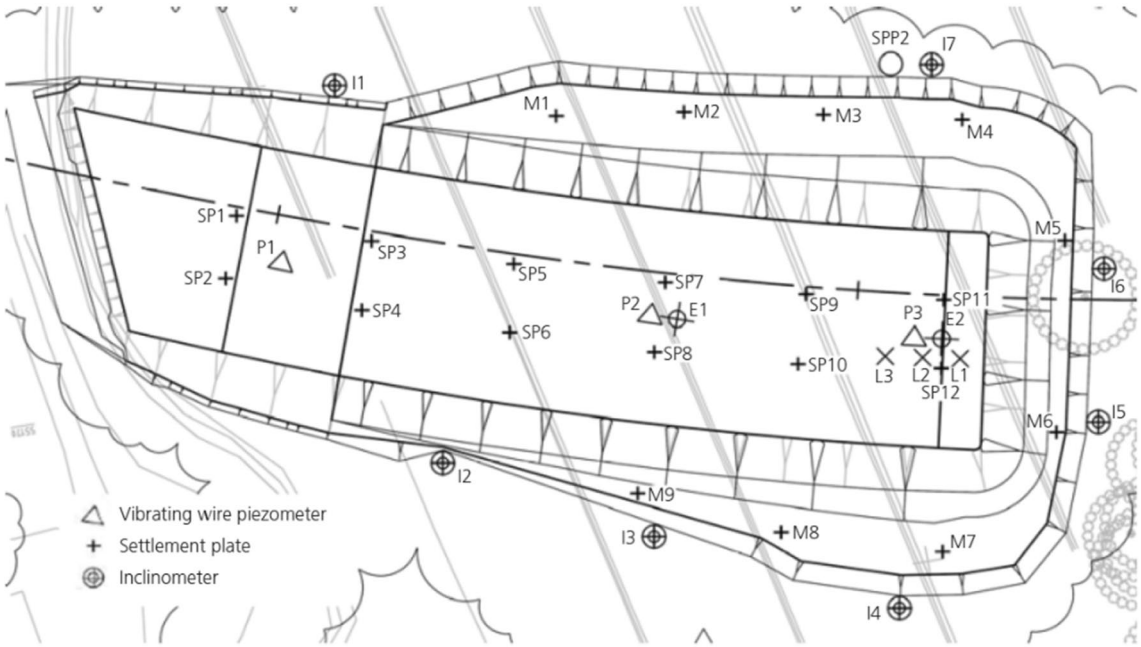

Fig. 7 Instrumentation layout at the test embankment (not to scale) (Source: Indraratna et. al. [11])

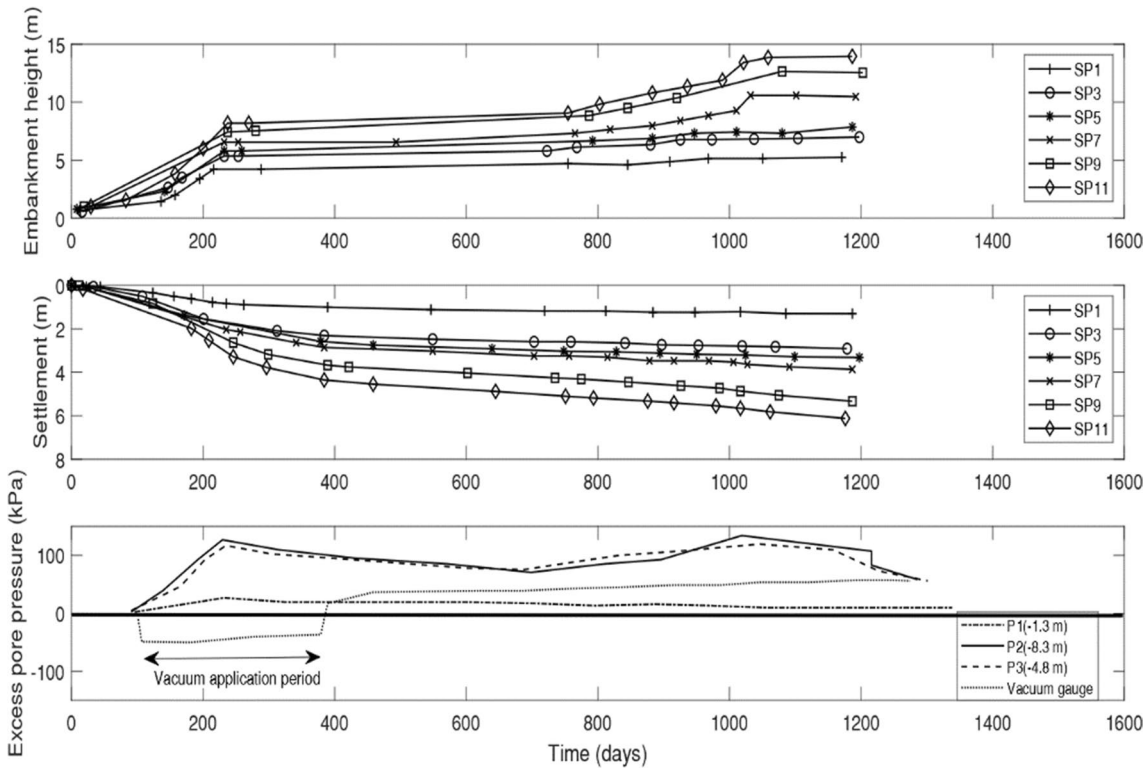

Fig. 8 Settlement and excess pore pressure result with embankment construction schedule (data sourced from Indraratna et. al. [11])

surcharge load and soft clay thickness (2.7–6.7 m). At the position of SP11, the clay thickness was higher; therefore, the maximum vertical strain is noted.

The excess pore pressure dissipation after the embankment construction was higher in the vacuum area compared to the non-vacuum area. In the non-vacuum area,

Table 5 Bottom level of the soft clay layer at the positions of each settlement plate [11]

Settlement plate	The bottom level of soft clay layer in m (RL)
SP1, SP2	2.7–6.7
SP3, SP4	6.7–9.7
SP5, SP6	9.7–11.7
SP7, SP8	11.7–14.7
SP9, SP10	14.7–17.7
SP11, SP12	20.7–24.7

the embankment height could not be raised more than 4 m; whereas, the embankment height was increased to 8 m in the vacuum-applied areas. In the regions where the vacuum was applied, the peak excess pore pressure (120 kPa) was lower than the applied surcharge load (160 kPa). This was due to the suction provided by the vacuum, which increased the effective stress in soft soil layers.

The lateral displacement at the embankment's edge was monitored by inclinometers I1, I2, I3 and I4. Inclinometer I1 was positioned at the border of section A; whereas, other inclinometers (I2-I4) were located at the edge of section B. Figure 9 shows the measured lateral displacement and lateral displacement normalized by embankment height plotted against depth. The application of vacuum during preloading had a substantial effect in reducing lateral displacement.

A rapid increase in lateral displacements was observed for the first 400 days which became stagnant during the rest period. When the second stage of embankment construction commenced (i.e. after 750 days), there was a significant rise in measured lateral displacements from the inclinometers I3 and I4. As shown in Fig. 10, the maximum lateral displacement with the surface settlement shows that maximum lateral displacements in the vacuum area are less than in the non-vacuum area.

Effectiveness of Vertical Drain Systems

The performance of a vertical drain system depends on the drain length (l_d), the height of the surcharge load (H) and the diameter of drain influence zone (d_e). Therefore, a normalised parameter (β) which captures the effect of drain length, surcharge load height, and drain influence zone, was introduced to study the efficiency of the drain system in varied site conditions.

$$\beta = \frac{l_d H}{d_e^2} \tag{1}$$

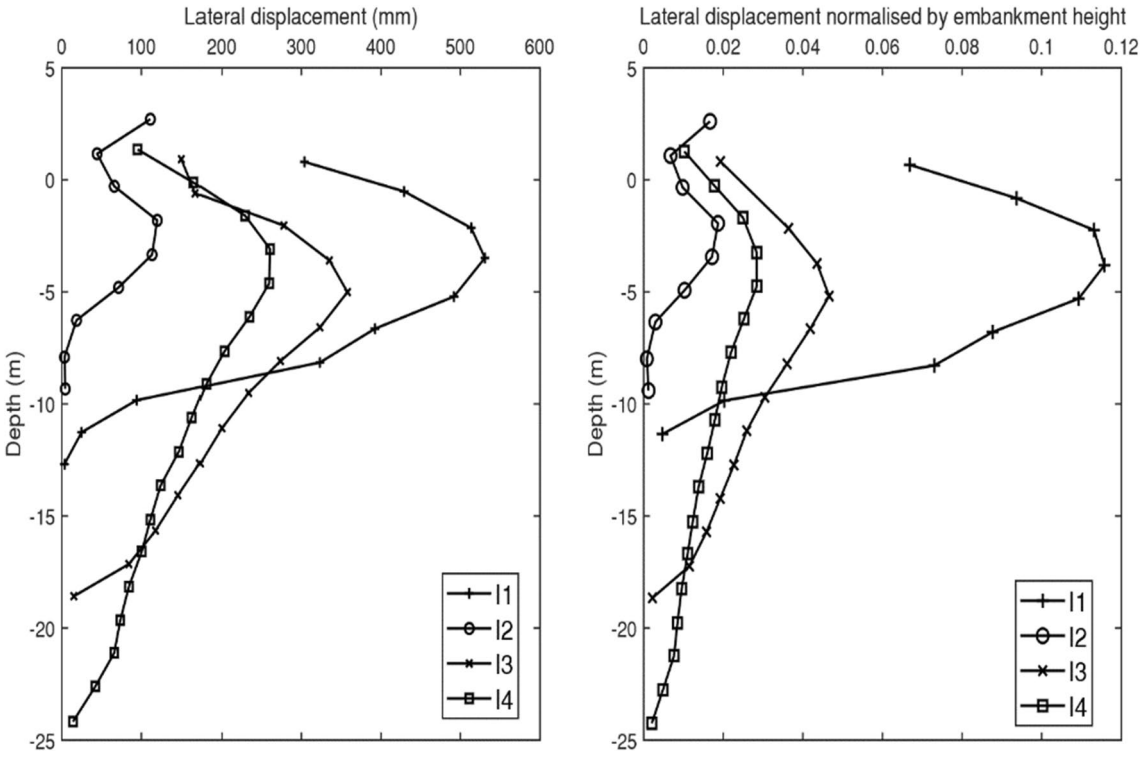

Fig. 9 Measured lateral displacements and lateral displacements normalized with embankment height after the first stage of construction (data sourced from Indraratna et. al. [11])

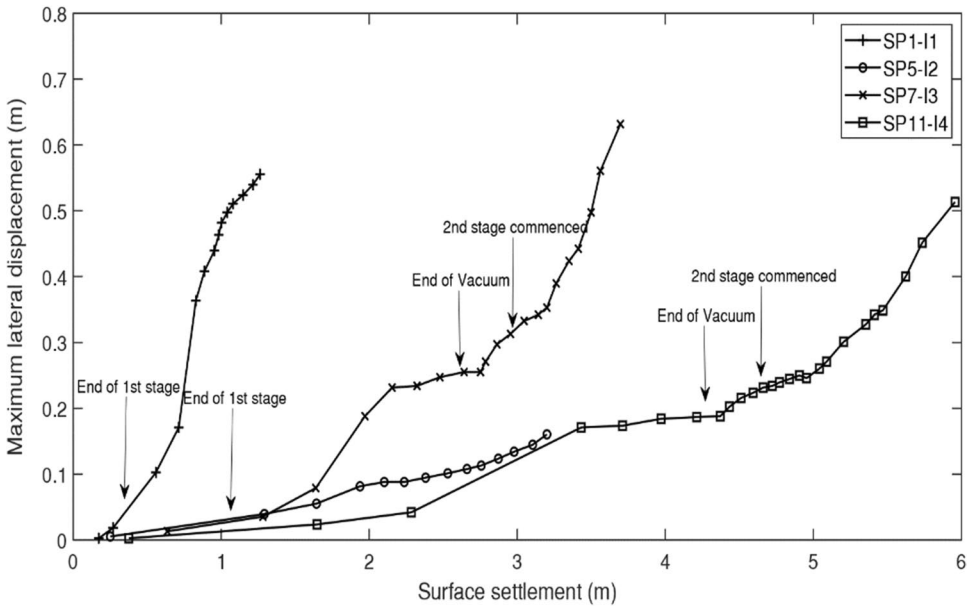

Fig. 10 Relation between measured lateral displacements and surface settlements (data sourced from Indraratna et. al. [11])

The dimensionless parameter, β, was used to compare the performance of vacuum-assisted surcharge preloading with the non-vacuum areas (as the settlement pattern was the same for these areas). Figure 11 compares the performance based on surface settlement and vertical strain rate. It can be inferred that the vacuum consolidation reached the highest efficiency in the area of SP3 due to the lower soft clay thickness (6.7–9.7 m) in that area compared to other vacuum sites. In the locations where the clay layer thickness exceeded 12–15 m (SP7, SP9 and SP11), there was a decrease in the β parameter and vertical strain rate, thus indicating that increased thickness of the clay layer can restrict the efficient propagation of vacuum in the lateral directions.

Sandgate Rail Grade Separation Project

The eastern part of Kooragang Island near Newcastle, New South Wales, was a major coal export port and was connected to the Sandgate through a railway line across the Hunter River. Due to the increasing freight traffic to the port, new railway lines were constructed along the main line in Sandgate, which acts as a junction for freight traffic from the port and passenger traffic on the main line. The subgrade consisted of very soft clays that needed further ground improvement before commencing construction. Prefabricated vertical drains were considered to improve the track's soft formation. Due to the time constraints for track construction, the dead load from the track and live loads

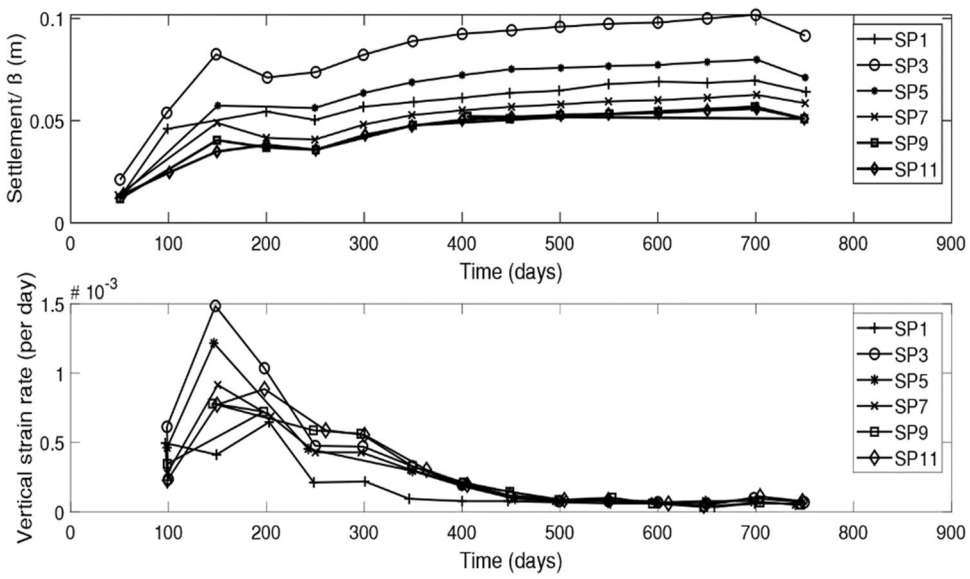

Fig. 11 Surface settlement and vertical strain rate comparison (data sourced from Indraratna et. al. [11])

from trains were used as surcharges instead of the traditional embankment surcharge. This case study highlights the importance of Class-A predictions that were carried out using numerical analysis to determine the length and spacing of PVDs.

Site investigations conducted at the site using boreholes, piezocone, Cone Penetration tests, and in situ vane shear tests indicated a soft compressible soil deposit of thickness 4–30 m underlying the existing embankment. Under the soft soil layer, a soft residual soil layer was encountered, followed by shale bedrock. Further, laboratory index tests from field samples reported that the water content of the soft clay layer was close to its liquid limit with an undrained shear strength of 10–40 kPa [35].

Class A Predictions with Finite Element Modelling

Numerical analysis was conducted using the finite element software PLAXIS to simulate the behaviour of the track subgrade using a coupled flow-deformation analysis. The track was modelled in 2D plane strain with triangular elements, as shown in Fig. 12. The ballast and fill layers were modelled using the Mohr–Coulomb criterion; while, the soft soil layers were modelled using the modified cam clay theory. To simulate PVDs, interface elements with zero excess pore pressure were used, and four vertical drains were considered for the analysis. The ballast layer was regarded as free draining, and the bottom boundary was set as a non-displacement boundary at a depth of 20 m from the surface. The lateral boundary was chosen to be 45 m away from the embankment edge. Conversion of axisymmetric to 2D conditions was adopted to conduct the multi-drain analysis. The conversion details can be found elsewhere [35].

The predictions of settlements and excess pore-water pressures from the numerical model are shown in Figs. 13a and b. From the finite element studies, vertical drains assisted with 90% consolidation in the first year compared to 20 years in the case without PVDs (Fig. 13a). Additional drainage via PVDs also dissipated 60% of pore pressure in the first three months and was beneficial in curtailing lateral displacement (Fig. 13b). A closer PVD spacing of 1.5 m performed better than 2 m spacing in accelerating the consolidation process. However, the difference in performance was found insignificant, and 2 m spacing was used to minimise the costs.

Installation of PVDs and Instrumentation

The PVDs of 8 m in length at a spacing of 2 m were installed in a triangular pattern using a steel mandrel. The PVDs were 100 mm wide and 4 mm thick, with a discharge capacity of 3×10^6 L per year. Different field instrumentations, such as settlement plates, inclinometers, and vibrating wire piezometers, were installed to monitor the consolidation process and the resulting track settlements. The field data were considered essential to assess the safety and suitability of the track, verify the design recommended, and improve the guidelines for future works with vertical drains. The field instrumentation data were also used to compare the results from the finite element analysis carried out as part of Class A prediction.

Comparison of Class A Predictions and Field Data

Immediately after the PVD insertion, the track was constructed, and the train load (25-ton axle load) at a low speed was applied as the external surcharge due to the time constraint. After a year of track operation, the field data were compared with the Class-A predictions. It was observed from Fig. 14a that the Class A predictions and field results of settlements at the centre of rail lines showed good agreements with each other. In addition, the track lateral displacements observed in the field also agreed with the predictions (Fig. 14b).

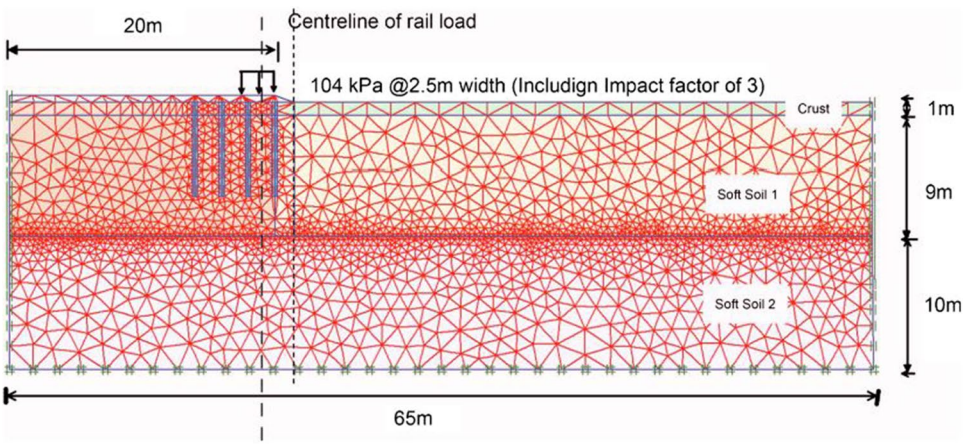

Fig. 12 Cross section of rail track and subgrade (source: Indraratna et. al. [35])

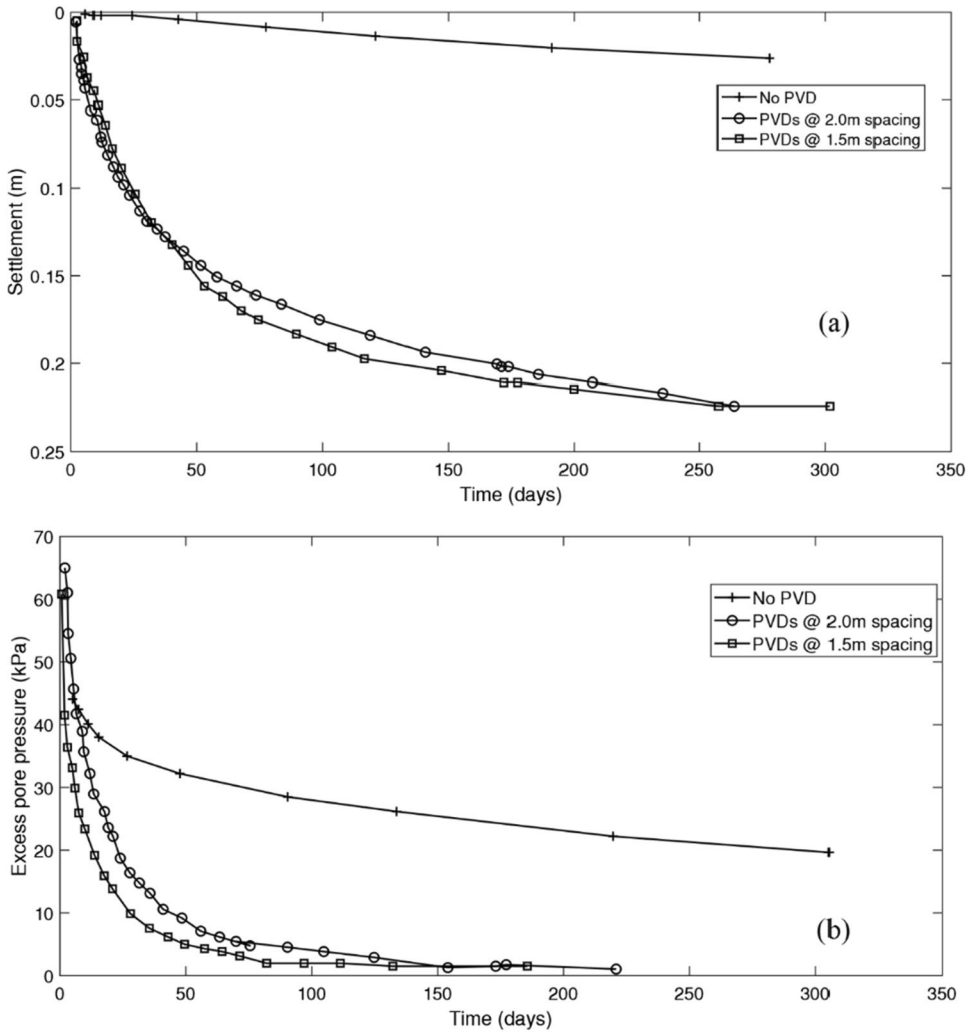

Fig. 13 Plot depicting **a** surface settlement at the centre line of rail load **b** excess pore pressure dissipation at 2-m depth at the centre line of rail track (data sourced from Indraratna et. al [35])

Recycled Ballast with Geosynthetic Reinforcement at Bulli, NSW

In addition to improving subgrade soils for the construction of road and rail infrastructure, a number of field studies were conducted to improve the performance of railway ballast and minimise ballast degradation using different artificial inclusions. An experimental track section was built at Bulli, NSW, with sponsorship from Sydney Trains (formerly RailCorp) to examine the performance of recycled ballast along with a geocomposite layer (geogrid bonded with non-woven geotextiles) [20]. Laboratory investigations using large scale cubical triaxial apparatus reported that the geocomposite layer not only provided stabilisation of recycled ballast when compared to standard geogrids but also was effective in preventing the migration of subgrade fines and capping material into the ballast layer [13, 19].

Site Characteristics and Track Construction

The experimental track section was constructed between two turnouts at Bulli with a total track length of 60 m, divided into four sections in which different combinations of fresh ballast, recycled ballast, and geocomposites were used, as shown in Fig. 15. The track substructure included 300 mm of ballast layer and 150 mm of capping layer. Fresh and recycled ballast was sourced from Sydney Trains following the technical specification TS 302 (Rail Infrastructure Corporation of NSW 2001a). The geocomposite layer consisted of a bioriented geogrid with rectangular apertures (size = 40 mm × 27 mm, peak tensile strength = 30 kN/m) placed over a non-woven geotextile of 2 mm thickness. Other specifications of the geocomposite are mentioned elsewhere in Indraratna et. al. [20]. The subgrade conditions at the track location were investigated using test pits and cone penetrometer tests. The

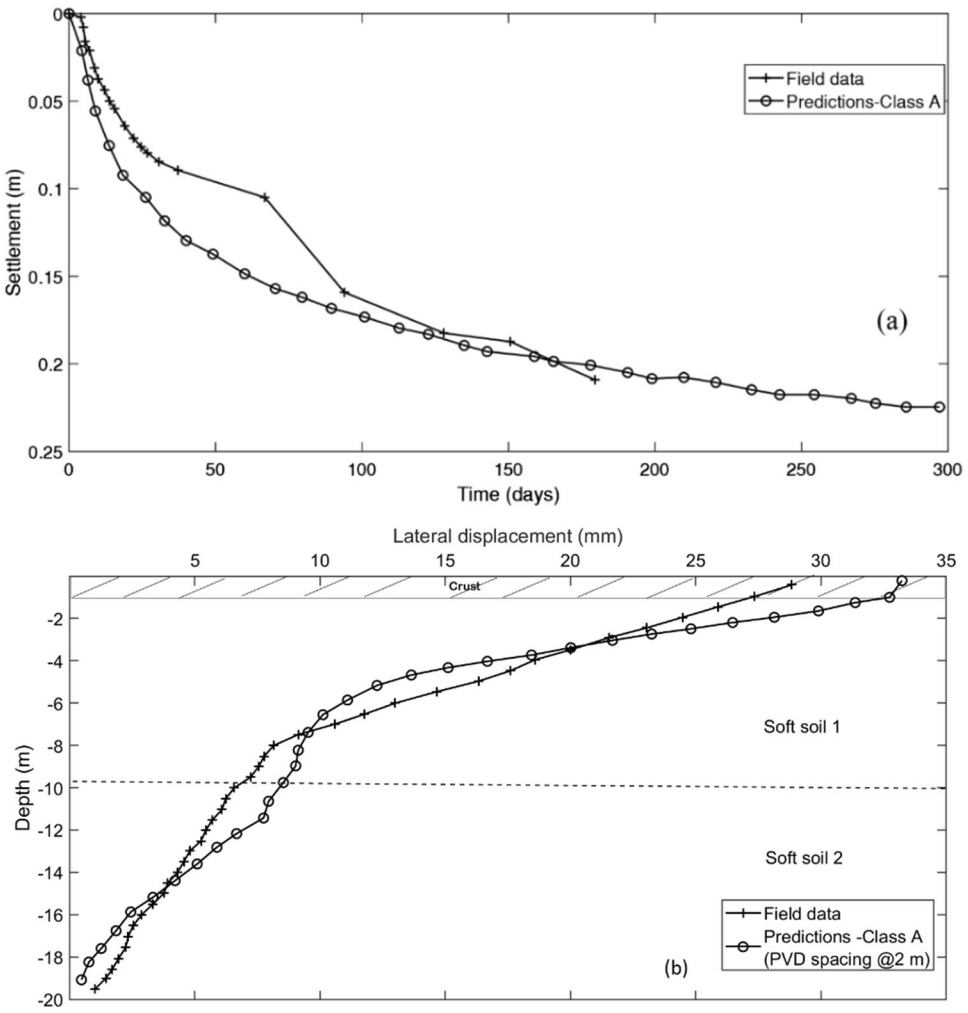

Fig. 14 Predicted and measured **a** consolidation settlements at the centre line of railway tracks **b** lateral displacement profiles near embankment toe at 180 days (data sourced from [35])

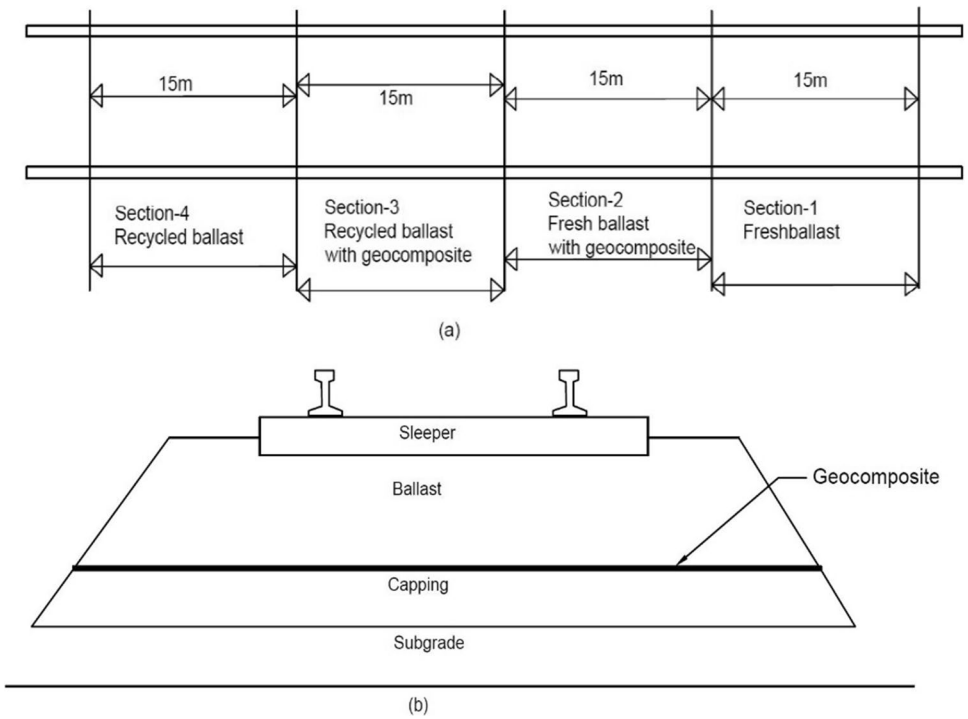

Fig. 15 Schematic of **a** Plan view of track showing different trial sections **b** Cross section of track (modified after Indraratna et al. [20])

subgrade was comprised of a stiff over-consolidated silty clay layer with shale cobbles and gravels underlain by a highly weathered sandstone bedrock. The depth of bedrock was reported as 2.3 m in Sect. 4, while its depth increased gradually towards Sect. 1.

Field Instrumentation

Three types of instruments were installed at the track site: settlement pegs and displacement transducers to measure deformations in vertical and lateral directions, and pressure cells to measure cyclic vertical stresses in the track, as shown in Fig. 16. The settlement pegs and displacement transducers were placed at two depths: at the sleeper-ballast

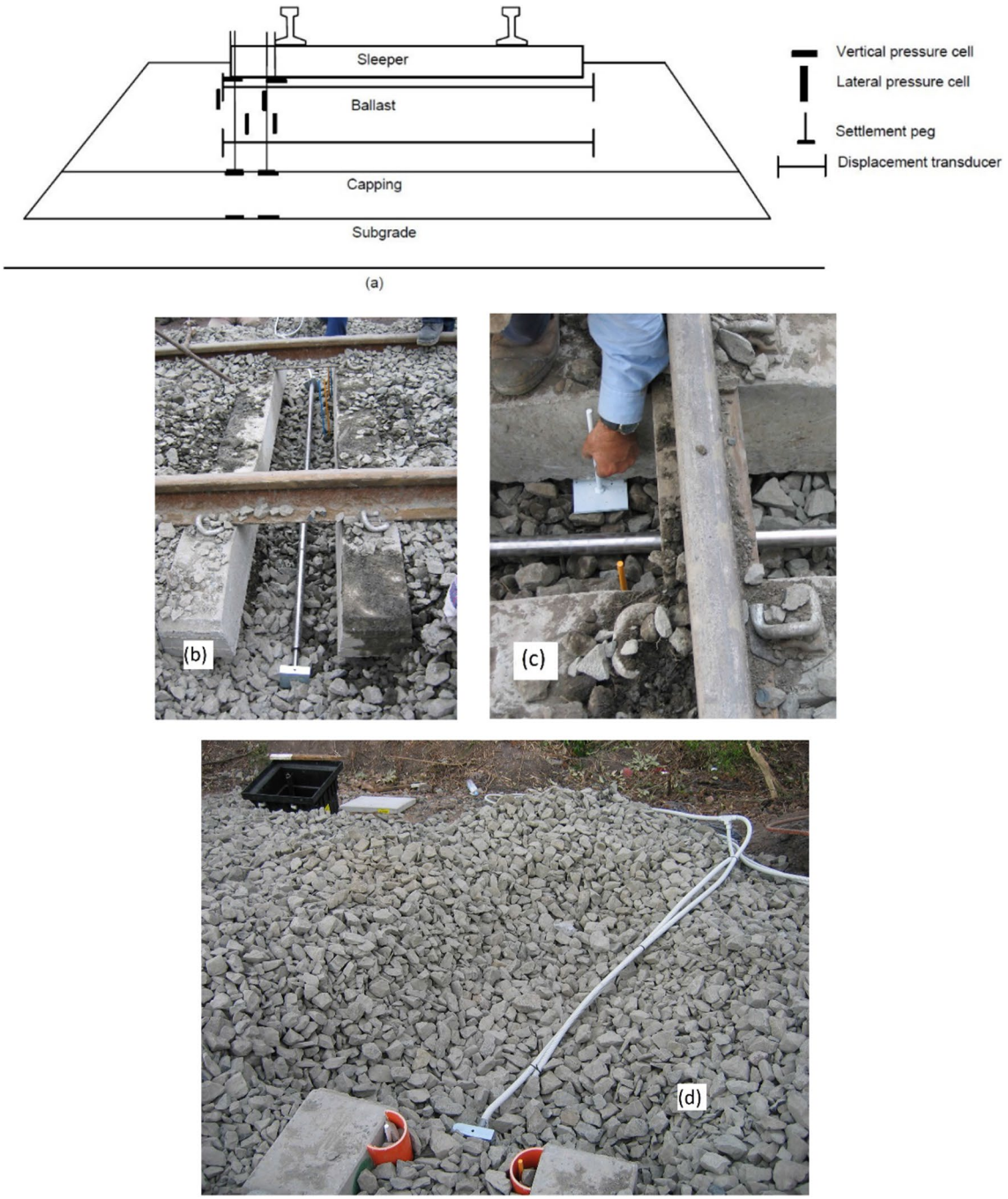

Fig. 16 Field instrumentation at Bulli: **a** Schematic of all instruments **b** Displacement transducer, **c** Settlement pegs **d** Protective casing for cables (modified after Indraratna et. al. [20])

interface and ballast-capping interface, both underneath the rail and near the edge of the sleeper. Traditionally displacement transducers are used for measuring vertical displacements; however, these were used to measure transient lateral track movements (See Fig. 16a). A 2.5 m long protective casing was provided to displacement transducers to prevent damage from ballast aggregates and moisture ingress. Six vertical pressure cells were used at the three interfaces, i.e. sleeper-ballast, ballast-capping, and capping-subgrade; while, four lateral pressure cells were used to monitor in situ lateral stresses in the ballast layer. All the electrical cables were connected to a data acquisition system securely fixed at a central location adjacent to the track.

A manual surveying technique was used to measure the vertical position of settlement pegs at different time intervals for 17 months. Data from displacement transducers and pressure cells were recorded using a manual trigger mechanism for each train passage, and the data logger was operated at a maximum frequency of 40 Hz. To correlate the deformations recorded by the data logger (in time scale) with respect to the number of loading cycles, the annual rail traffic (in Million Gross Tonnage, MGT) and axle load (P_t) were transformed into $N_t = 10^6/(P_t * N_a)$, where N_t is a number of load cycles per MGT and N_a is the number of axles in each load cycle. For an annual traffic of 60 MGT, a 25 T axle load with four axles per cycle gives 600,000 load cycles per MGT, and this calculation was used for analysing the results.

Field Data Interpretation

Stress in the Track Layers

The peak cyclic vertical and lateral pressures at different depths of ballast underneath the rail recorded for passenger and coal trains travelling at 60 km/h in Sect. 1 (i.e. fresh ballast without geocomposites) are shown in Fig. 17. The passenger and coal trains had an axle load of 20.5 and 25 t, respectively. As expected, the vertical and lateral stresses recorded under passenger trains are lower than that of a coal train due to a lower axle load. The vertical stresses attenuated with depth, and the gradient of stress attenuation is higher in the ballast layer when compared to that in the capping layer. As the number of load cycles increased, the vertical stresses increased by approximately 10% at all depths, and this can be attributed to the reduction of the bearing capacity of ballast as degradation increases. The recordings show that the lateral stresses recorded for both trains are lower than that of the vertical stresses, therefore producing the potential for large shear strains in the track layers. In contrast to vertical stresses, there is no significant depth attenuation observed in lateral stresses.

Deformations

Ballast vertical deformations are computed by subtracting the settlement peg readings at the ballast-capping interface from the readings at the sleeper-ballast interface. The vertical deformation of the ballast layer with the number of loading cycles at different track sections is plotted in Fig. 18. As observed, all sections of the track showed increased deformations with time, i.e. an increase in loading cycles. The magnitude of deformations in fresh ballast was found to be higher than that of recycled ballast and much of this difference occurred in the first few cycles. This can be due to the lower angularity of recycled ballast when compared to fresh ballast yielding less particle breakage during the initial phases of loading. However, the benefits of geocomposites

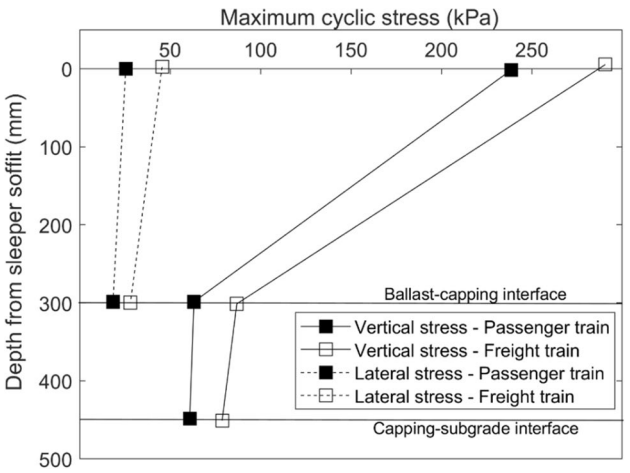

Fig. 17 Stress distribution in ballasted railway track (depths underneath rail) under different trains (data sourced from Indraratna et. al. [20])

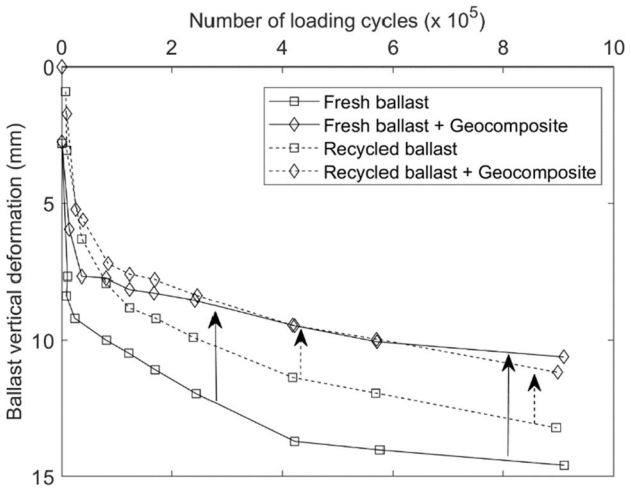

Fig. 18 Vertical deformation of ballast in fresh ballast and recycled ballast sections with and without geocomposites (data sourced from Indraratna et. al. [20])

were found maximum in fresh ballast, which showed a 33% reduction of vertical deformations compared to 9% in recycled ballast. Similarly, a 49% reduction in lateral deformations was observed for geocomposite with fresh ballast; while, 11% reduction was recorded with recycled ballast, signifying that geocomposites can improve lateral stability. Nevertheless, the environmental benefits are evident by using recycled ballast while its performance can be enhanced by geocomposite reinforcement. This field study considered only one type of geocomposite due to constraints with time. These limitations were addressed in the field study conducted in Singleton, NSW in 2014 where different types of geocomposites were tested on both soft and hard subgrades along with other research innovations.

Performance Evaluation of Geocomposites and Shock Mats at Singleton, NSW

Earlier field investigations from Bulli showed that geocomposites work effectively to reduce both vertical and lateral deformations in the ballast layer, however, the type of geocomposites and subgrade conditions are limited to a particular type. As an extension, different types of geosynthetics, along with a shock mat were tested in different subgrade conditions at Singleton, NSW. This track was owned and operated by Australian Rail Track Corporation (ARTC) and was located inland in the Hunter Valley region of NSW.

Site Characteristics and Track Construction

Subsurface exploration at the site was done using 33 boreholes, eight dynamic cone penetration tests, and 11 standpipe piezometers and three subgrade conditions were selected. These included medium to high-strength siltstone rock, a flood plain with soft alluvial deposits, and a reinforced concrete bridge supported by piled abutments [21]. The flood plain consisted of silty clay (7–10 m thick) and medium dense sand-silty clay of 7–9 m thick layers underlain by medium-strength siltstone. In addition to ballast (300 mm) and capping (150 mm) layers, a 500 mm structural fill was placed on the subgrade. Four types of polypropylene geogrids, a geocomposite layer, and a shock mat were installed at the ballast-capping interface in 8 different sections, as given in Table 6. More specifications of these inclusions are reported in Nimbalkar and Indraratna [21].

Field Instrumentation at Singleton

In this track, settlement pegs and pressure cells were installed at different layer interfaces to monitor deformations and stresses, respectively. In addition, high-precision sensors such as strain gauges were installed in the track to monitor longitudinal and transverse strains mobilised in geogrids and geocomposite layer as shown in Fig. 19a. These strain gauges are temperature resistant, could measure up to 15% strains, and were installed on the top and bottom of the geogrids at 3 spatial locations, i.e. below the edge of the sleeper, below the rail and near the centre of the track. To measure the lateral and vertical deformations in the ballast layer, a group of linear variable differential transformers (LVDTs) was mounted on a custom-made frame near the shoulder, as shown in Fig. 19b. As observed from Fig. 19b, this setup allows the measurement of transient lateral movements at different depths of ballast layer. Detailed site instrumentation drawings are presented in Nimbalkar and Indraratna [21].

For the standard sleeper width of 240 mm, a train speed of 100 km/h would require a data acquisition system with a minimum acquisition frequency of 350 Hz for the instrumented sleeper to sufficiently capture the effects of a passing wheel. It was reported in earlier field trials at Bulli that a data acquisition system with 40 Hz could not capture the data entirely and data loss was observed. To minimise this, the Singleton field trial was equipped with an advanced data acquisition system to obtain data at a 2 kHz frequency. Further, each load cycle in this study was considered equivalent to one axle instead of one bogie used at Bulli.

Table 6 Type of inclusions installed in railway track at Singleton, NSW

	Subgrade conditions	Type of inclusion (aperture size)
Section-1	Alluvial deposit	GG-1 (44 × 44 mm)
Section-2	Alluvial deposit	GG-2 (65 × 65 mm)
Section-3	Alluvial deposit	GG-3 (40 × 40 mm)
Section-4	Alluvial deposit	GC-1:GG-4 (31 × 31 mm) + Non-woven geotextile
Section-5	High strength siltstone	GG-3
Section-A	Alluvial deposit	Standard section for comparison
Section-B	Concrete Bridge deck	Shock mat (polyurethane elastomer, 10 mm thick)
Section-C	High strength siltstone	Standard section

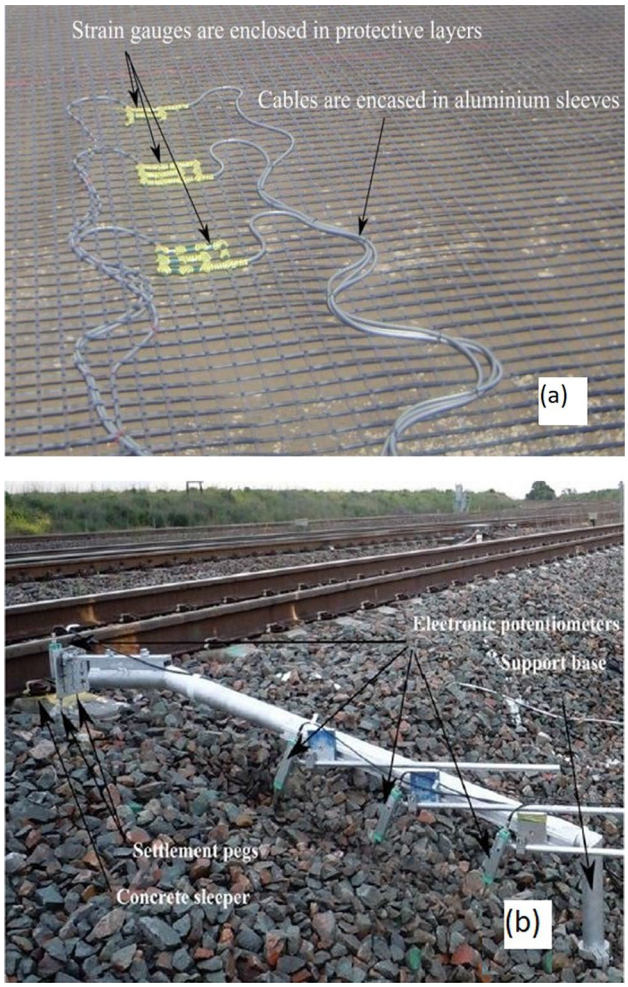

Fig. 19 Pictures of **a** strain gauges installed on geogrids **b** LVDTs mounted on displacement measurement frame (Source: Nimbalkar and Indraratna [21])

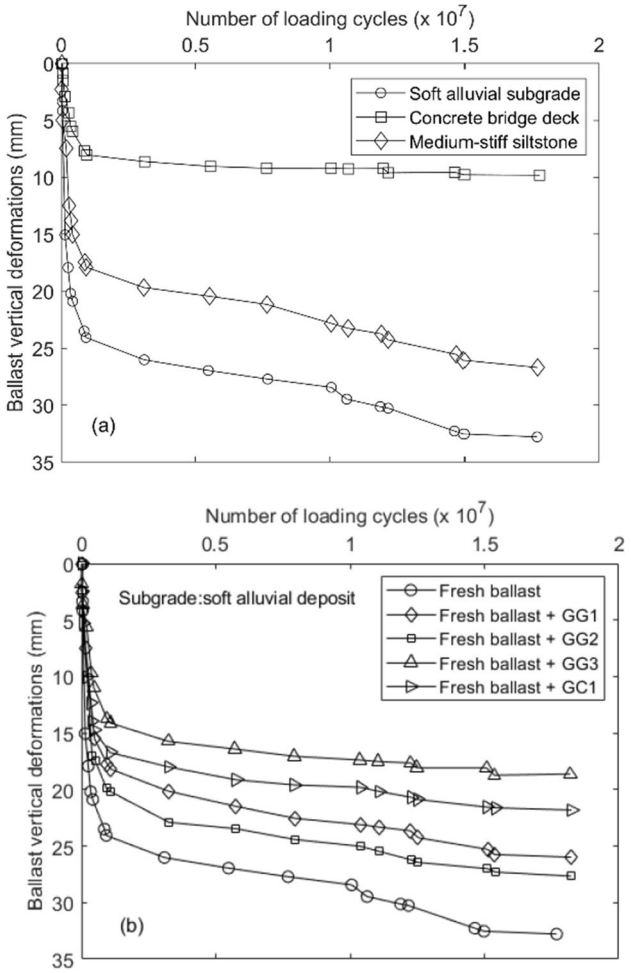

Fig. 20 Deformations of ballast layer with number of loading cycles for **a** different subgrade conditions **b** Different geosynthetic inclusions on soft alluvial deposits (data sourced from [21])

Performance of geogrids and geocomposites

The track at Singleton was used by freight trains of two-axle loads (25 and 30 T) at different train speeds. The vertical deformations of the ballast are shown in Fig. 20a. Similar to ballast deformations in the laboratory, the ballast layer experienced large deformations in the first 10,000 load cycles, after which the increment rate gradually reduced. After the initial phase, it was observed that ballast deformations on the soft subgrade were 30% higher than those on the hard subgrade. The ballast on the concrete bridge deck experienced only about 9 mm deformations which are 60% less than that on hard subgrade. These low deformations on the concrete bridge deck are predominantly because of shock mats placed underneath the ballast. Further, the lateral restraint of ballast by bridge-side barriers reduced vertical deformations when compared to other sections with free shoulders. The influence of different geogrid inclusions on ballast deformations for soft subgrades is shown in Fig. 20b. The results indicated that geogrid reinforcement reduced ballast deformations, and GG-3 performed better than all other types, including geocomposite layer, providing maximum reinforcement. It was interesting to note that the aperture size of GG-3 was close to the optimum aperture size (1.1 d_{50}=40 mm) reported by laboratory investigations and better performance compared to other geogrids, even with a non-woven geotextile inclusion. Further, Nimbalkar and Indraratna (2016) reported that higher transverse and longitudinal strains were mobilised in GG-3, indicating maximum resource utilisation.

Track Dynamic Response

Figure 21a and b shows the peak dynamic stress and transient vertical displacements at the sleeper-ballast interface at different locations, respectively. In all track sections, the dynamic stresses increased as train speeds increased for the

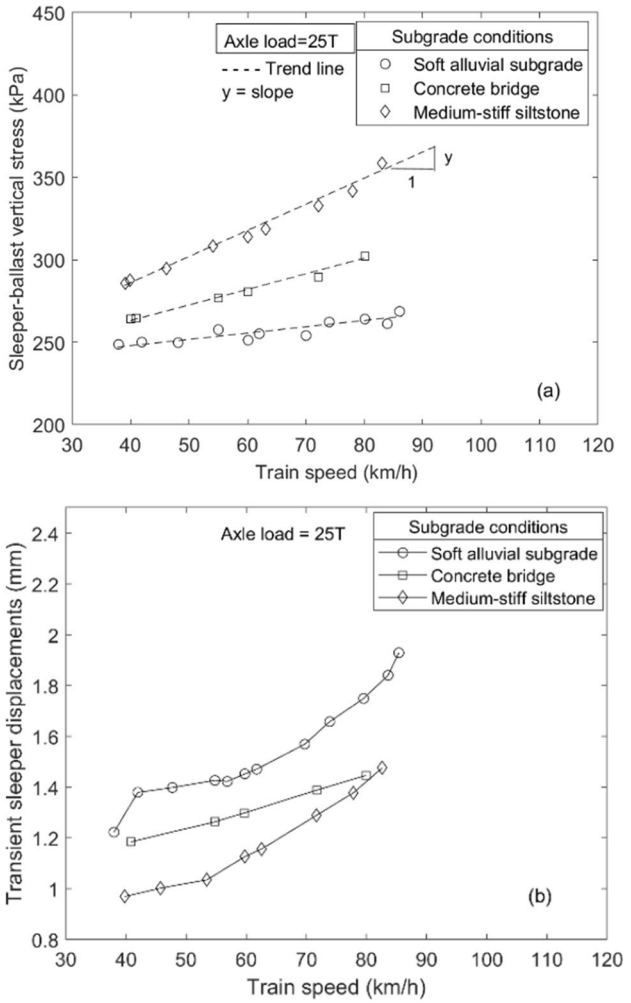

Fig. 21 **a** Dynamic vertical stresses under sleepers and **b** transient sleeper displacements at Singleton for different subgrade conditions (data sourced from Nimbalkar and Indraratna [21])

same axle load. This dynamic amplification is due to the propagation of surface waves in the track substructure layers, and the wave propagation characteristics are directly related to subgrade conditions. The magnitude of stresses was found to be maximum for the track on medium-stiff siltstone and minimum for the track on soft alluvial deposit (see Fig. 21a). This high amplification on hard subgrades can be attributed to the reflection of stress wave from stiff siltstone layers, which has higher shear modulus compared to the other substructure layers above it. Despite the higher shear modulus of reinforced concrete, the vertical stresses recorded on bridge decks were lower than those for stiff subgrade conditions. The shock mats placed on the bridge deck acted as an energy-absorbing layer attenuating the dynamic effects of wave reflection on stiff subgrades, thus reducing the dynamic vertical stresses. The amplification of stress with train speed curves was found to be linear, and the dynamic amplification factor, i.e. the slope of trend line, was higher on stiff subgrades (1.4) and reduced to 0.95 and 0.42 on the concrete bridge deck and soft subgrade, respectively.

Further, when the transient displacements were plotted against train speeds (see Fig. 21b), it was observed that the displacements were maximum for the track on soft alluvial deposits and minimum on hard subgrades. This is expected as stiffness and displacements are inversely related to each other. However, the amplification trend of displacements was found to be nonlinear in contrast to stresses; while, the apparent amplification was higher on soft subgrades.

Large-Scale Heavy Haul Track Testing Facility

The case studies discussed in the previous sections demonstrate that an extensive amount of effort, time and money must be invested in conducting full-scale field trials on active railway tracks. Moreover, it is not feasible to modify the test tracks after commissioning to incorporate any design modifications or new research innovations. Any such modifications would require the whole track construction process to be repeated. In view of this, a prototype test facility was built at Russell Vale, 80 km south of Sydney, which can simulate the axle loading and track in situ boundary conditions for standard gauge heavy haul tracks. This National Facility for Heavy-haul Railroad Testing (NFHRT) was built through a collaboration of multiple Universities, Industry organisations and the Australian Research Council under the leadership of the first author. This case study presents some of the critical aspects of NFHRT and the performance of a standard test compared with Bulli and Singleton field studies.

Specifications of NFHRT

A full-size (1:1 scale) instrumented track section of 6 m length was constructed on a test pit with 6 m width and 2.3 m depth to minimise the boundary effects that are generally associated with unit cell type large-scale testing facilities. The schematic and real-life picture of the facility is shown in Fig. 22a and b, respectively. Vibration insulation has been provided to the edges of the test pit through 900 mm thick reinforced concrete walls and 600 mm thick concrete floor to prevent vibrations from propagating to other nearby facilities. The equivalent load from a typical freight wagon bogie was simulated in NFHRT using four dynamic hydraulic actuators with a capacity to apply up to 40 T axle loads to 200 km/h. These hydraulic actuators are mounted on a loading frame and controlled using the hydraulic servo-controlled system, as shown in Fig. 22a. All the actuators were controlled through a computerised operating system linked to a robust data acquisition system. The four actuators were

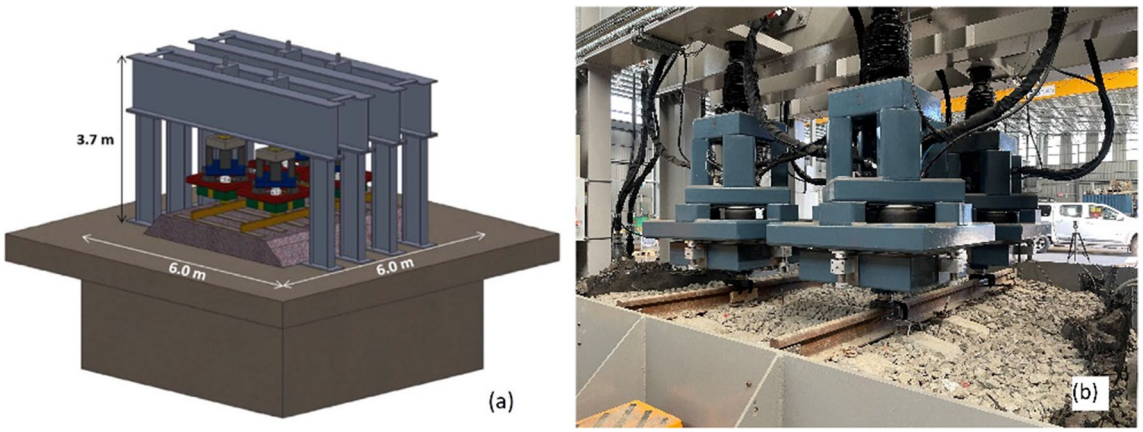

Fig. 22 **a** 3D Schematic of NFHRT **b** Real-life picture of mounting frame with actuators resting on track (Source: Indraratna et al. [38])

paired into two axles (front and rear) which operate at a phase difference equivalent to the simulated train speed based on Indraratna et al. (2011).

Track construction and instrumentation

To simulate field conditions of railway tracks on soft alluvial subgrades, the test pit was filled and compacted to ground level by drainage layer, subgrade, structural fill, and capping layer in sequence from the bottom of the pit. Material characteristics of each layer and their design thickness are summarised in Table 7. On top of the capping layer, 300 mm thick fresh ballast obtained from Bombo quarry in NSW was placed and compacted, overlain by the standard rail-sleeper assembly. The construction of capping and ballast layers was done in accordance with AS 1289.5.1.1 and AS1289, respectively.

Many instruments were installed in the track during construction, including settlement pegs, pressure cells, and high-precision sensors such as horizontal displacement transducers, pore pressure gauges, and soil moisture sensors as shown in Fig. 23. In addition, accelerometers were installed on rails and sleepers to measure accelerations during loading. The exact locations of all these instruments are given elsewhere in Indraratna et al. [38].

Data Interpretation

A 25 T axle load bogie with an applied frequency of 15 Hz (~60–80 km/h) was simulated in the facility up to 500,000 cycles. Figure 24a shows the average vertical settlement of two sleepers under each axle, measured by settlement pegs. The measurements showed that most settlements occurred in the first 50,000 cycles and the rate of increment in settlements reduced gradually with an increase in the number of loading cycles. Sleeper settlements from Bulli and Singleton field studies, along with large-scale cubical triaxial tests, were also plotted for comparison. In the initial 50,000 cycles, all measurements were in good agreement; however, the sleeper settlements in NFHRT at higher loading cycles are higher than those from laboratory testing but lower than those from field trials. Higher settlements in field trials are due to large depths of alluvial silty clay layers, i.e. 2.3–3 m at Bulli and 7–10 m at Singleton. While a large-scale cubical triaxial facility could not simulate these higher depths at the base resulting in boundary effects, a full-scale test in NFHRT was able to capture the depth effect satisfactorily, clearly highlighting the advantage of NFHRT. However, slight differences in NFHRT and field measurements can be due to external factors that are common in the field such as mixed axle loads (25 to 30 T), impact loads caused by wheel flats and rail corrugations, train acceleration-deceleration forces and seasonal moisture variations in subgrade layers.

Table 7 Materials used in NFHRT (data sourced from Indraratna et. al. [38])

Layer	Thickness (mm)	Properties
Drainage layer	75	Coarse-grained gravel overlain by a non-woven geotextile
Subgrade	795	Fine-grained CL type subgrade soil (w=20%, compacted in 4 layers to γ_{dry}=16.5 kN/m^3)
Structural fill	650	w=20%, compacted in 4 layers to γ_{dry}=18.5 kN/m^3
Capping layer	180	Sand-gravel mixture, compacted in 2 layers to γ_{dry}=19.5 kN/m^3

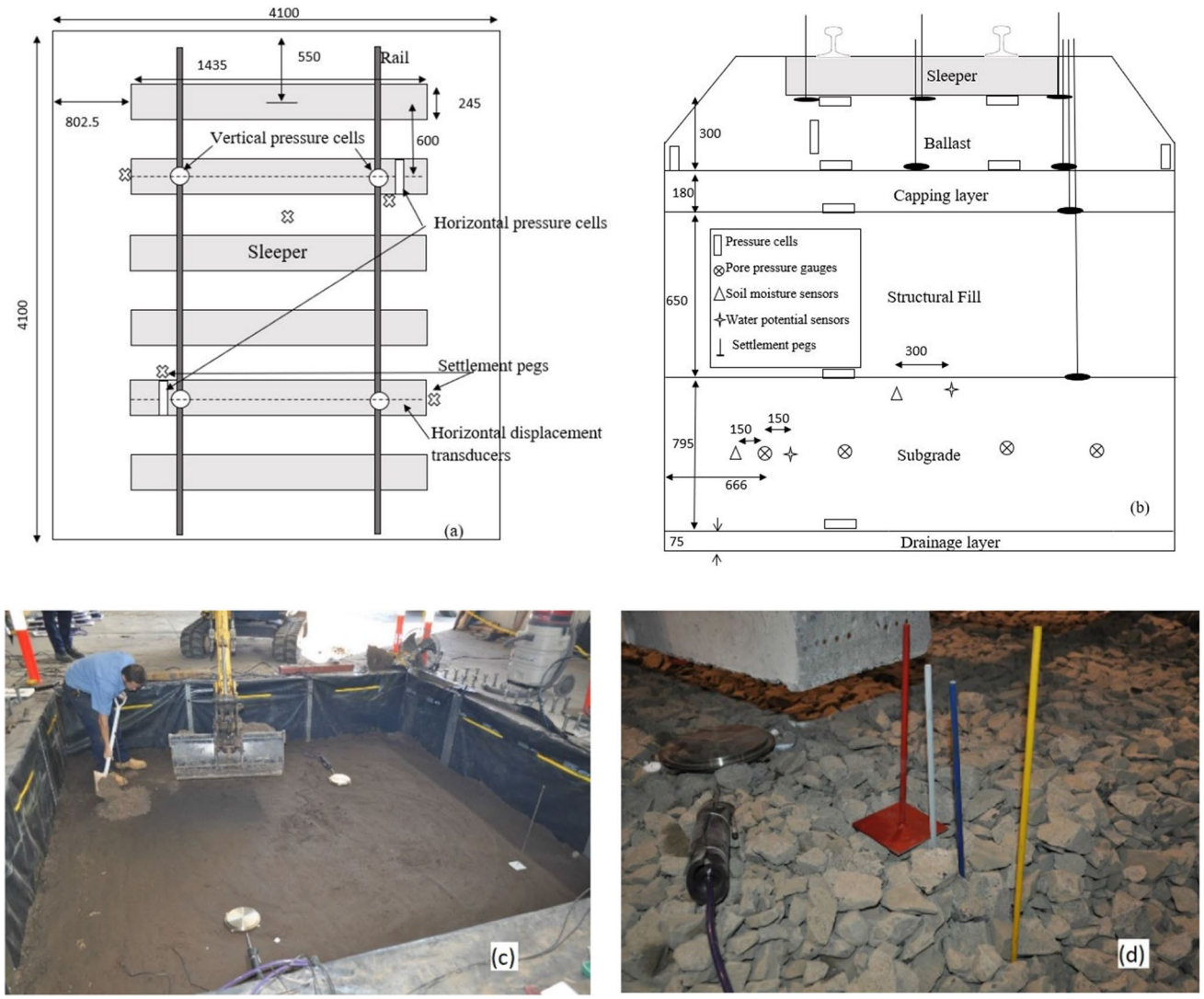

Fig. 23 **a** Plan view and **b** Cross section view of instrumentation at NFHRT **c** Installation of pressure plates in subgrade **d** pressure plates and settlement plates at sleeper base (sourced from Indraratna et al. [38])

Further, Fig. 24b shows the measured vertical stresses at different depths underneath the sleeper and compares them with field and lab studies. It can be observed that the vertical stresses attenuate with depth rapidly in the ballast layer and then gradually in subsequent layers. The peak vertical stress recorded was 225 kPa at the sleeper-ballast interface and 150 kPa at ballast-capping interfaces. The corresponding peak vertical stresses measured at Bulli were lower than the NFHRT measurements since the field stresses were measured for passenger trains (~ 19 T axle loads). Also, because of boundary effects in laboratory equipment were evident in high sleeper-ballast interface stress due to stress-wave reflection, while these wave reflection effects were not observed in full-scale tests conducted in NFHRT.

Challenges with Field Instrumentation

While conducting field trials, it is common that some of the installed instruments show erroneous measurements due to incorrect installation procedures, insufficient capacity of sensor measurements and insufficient protection of sensors and data cables from damage. For piezometers used in Port of Brisbane and Ballina case studies, the piezometers capacities are selected such that they can measure negative excess pore pressures (~ 70 kPa) that could occur due to the application of vacuum. In railway tracks, sharp angular ballast particles can easily damage any cables that are passing through the ballast layer and appropriate protective casing were used in Singleton and Bulli field studies to prevent such faults. Incorrect placement of sensors such as pressure cells could

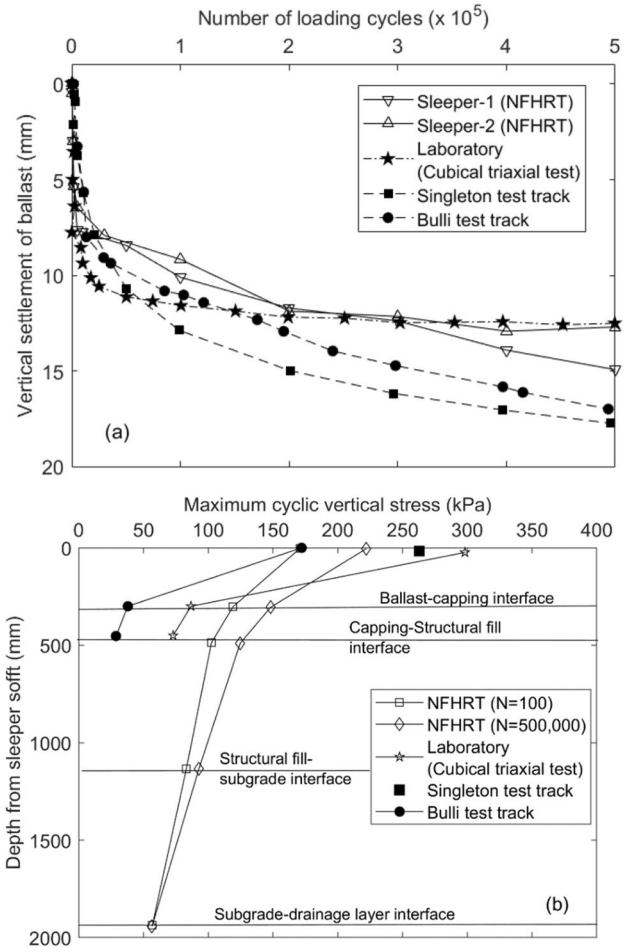

Fig. 24 Comparison of NFHRT test measurements with previous field and laboratory studies **a** Ballast settlement **b** Vertical stresses (data sourced from Indraratna et. al. [38])

also lead to wrong measurements, for e.g., the sensing face of the pressure cell should have sufficient contact with higher number of ballast particles to prevent stress concentrations and maintain accuracy of measurements [20, 21]. Further, the frequency of data acquisition becomes important while measuring the dynamic stresses and displacements under train loads, as lower frequency acquisition leads to loss of measurement data in terms of local minima and maxima. In such cases, it is essential to calculate minimum frequency based on the average train speed at the location to improve the quality of data.

In addition to incorrect installation procedures, interaction of some instruments with harsh conditions can also affect the accuracy of measurements. As observed in the Port of Brisbane and Ballina field cases, clogging of vibrating wire piezometers limited the capacity of the instrument to detect pore water pressures as expected. This trend was observed for much of the eastern coastal belt which is predominantly affected by Acid sulphate soil conditions which contain oxidisable pyrite layers at shallow depths in upper Holocene clay [6]. In such cases, data interpretation following fundamental concepts aided by supplementary numerical modelling plays a crucial role in identifying the erroneous measurements recorded by damaged instruments.

Conclusions

A number of field investigations involving several ground improvement techniques in transportation infrastructure were discussed in this paper through separate case studies. Different instrumentation procedures and analysis techniques were highlighted, explaining the importance of field measurements in monitoring the performance of embankments and railway tracks.

The use of field instruments like settlement plates, piezometers and inclinometers helped analyse the performance of PVDs to improve soft subgrades with vacuum-assisted preloading. Port of Brisbane and Ballina trial embankments showed that PVDs performed better in vacuum areas than non-vacuum areas. They were more effective in propagating the vacuum pressure to a greater depth. Vacuum-assisted preloading also showed a higher dissipation of excess pore water pressures, thus highlighting the effectiveness of vacuum consolidation. A settlement-based degree of consolidation (DOC) showed that DOC in the vacuum area was significantly higher compared to the non-vacuum areas. The surface settlement data, when analysed, indicate that the settlement increased with the clay layer thickness, embankment height and vacuum application. Furthermore, as the clay layer thickness increases, the effectiveness of PVDs reduce as thicker clay layer tend to reduce vacuum propagation in lateral directions. Inclinometer readings proved that vacuum pressure significantly helped in curtailing the lateral displacements and the stability of the embankment was greater with vacuum consolidation indicated by μ. The field trial at Sandgate proved that low-speed train loads could be used as an alternative for traditional embankment surcharge preloading at locations when time constraints are strict. Further, it was also evident that Class A predictions using appropriate numerical modelling techniques with laboratory-determined parameters can help design the PVDs. However, the effectiveness of Class A predictions can be compromised if the soil parameters needed for numerical predictions are not accurately measured from laboratory and in situ investigations.

Field investigations on railway tracks proved that geocomposites enhanced the performance of the ballast layer by reducing vertical and lateral deformations as well as the degradation of ballast aggregates. Maximum performance was observed when the aperture size of geogrids was closer to the optimum aperture size reported from laboratory

investigations. The use of recycled ballast was found to be a feasible solution when used along with geocomposites to maximize the utilisation of quarry materials and minimise further ecological damage. On concrete bridge decks, shock mats reduced the dynamic load amplification at higher train speeds while also reducing ballast breakage.

Full-scale track testing facilities such as NFHRT at Russell Vale reduce the amount of effort, time and money in repeating field tests and helps accelerate the research validation. Heavy haul track testing using NFHRT showed that the scale and depth effects are minimised when compared to traditional small-scale and large-scale laboratory testing. This provides an opportunity to investigate further the dynamic influence of different train loads on track layers and the use of innovative inclusions such as geogrids, geocomposites, shock mats, etc., and sustainable materials for enhanced stability and resiliency of railway tracks.

Acknowledgements The authors would like to acknowledge the financial assistance by the Australian Research Council (ARC) and Cooperative Research Centre (CRC) for Rail Innovation through various Linkage projects and the ARC Industrial Transformation Training Centre for Advanced Technologies in Rail Track Infrastructure (IC170100006). The financial and technical support from SMEC-Australia, Transport for NSW (Formerly known as Sydney Trains), ARTC (Australian Rail Track Corporation), Australasian Centre for Rail Innovation (ACRI), Douglas Partners, Soils wick, Menard Oceania, Port of Brisbane Corporation among others is acknowledged. The contributions of past and present research staff and doctoral students, namely, Dr. Trung Ngo, Dr. Sanjay Nimbalkar, Dr. Vinod S. Jayan, Dr. Fernanda Bessa Ferreira, Ms Fatima Mehmood, and Mr Soumyaranjan Mishra that are included in the contents of this keynote paper are also greatly appreciated. The salient contents of this Keynote paper have been published earlier in scholarly journals and reproduced herein with kind permission from Transportation Geotechnics, Canadian Geotechnical Journal, ASCE-JGGE, Computers and Geotechnics, among others.

Funding Open Access funding enabled and organized by CAUL and its Member Institutions.

Declarations

Conflict of interest The authors declare that they have no conflict of interest.

References

1. Indraratna B, Redana IW (2000) Numerical modeling of vertical drains with smear and well resistance installed in soft clay. Can Geotech J 37(1):132–145
2. Indraratna B, Singh M, Nguyen TT, Leroueil S, Abeywickrama A, Kelly R, Neville T (2020) Laboratory study on subgrade fluidization under undrained cyclic triaxial loading. Can Geotech J 57(11):1767–1779
3. Selig ET, Waters JM (1994) Track geotechnology and substructure management. Thomas Telford Publishing, London
4. Indraratna B, Bamunawita C, Khabbaz H (2004) Numerical modeling of vacuum preloading and field applications. Can Geotech J 41(6):1098–1110
5. Indraratna B, Attya A, Rujikiatkamjorn C (2009) Experimental investigation on effectiveness of a vertical drain under cyclic loads. J Geotech Geoenviron Eng 135(6):835–839
6. Indraratna B, Baral P, Rujikiatkamjorn C, Perera D (2018) Class A and C predictions for Ballina trial embankment with vertical drains using standard test data from industry and large diameter test specimens. Comput Geotech 93:232–246
7. Indraratna B, Rujikiatkamjorn C, Baral P, Ameratunga J (2019) Performance of marine clay stabilised with vacuum pressure: Based on Queensland experience. J Rock Mech Geotech Eng 11(3):598–611
8. Kelly RB, Sloan SW, Pineda JA, Kouretzis G, Huang J (2018) Outcomes of the Newcastle symposium for the prediction of embankment behaviour on soft soil. Comput Geotech 93:9–41
9. Indraratna B, Sathananthan I, Rujikiatkamjorn C, Balasubramaniam AS (2005) Analytical and numerical modeling of soft soil stabilized by prefabricated vertical drains incorporating vacuum reloading. Int J Geomech 5(2):114–124
10. Indraratna B, Rujikiatkamjorn C, Balasubramaniam AS (2013) Ground Improvement at the Port of Brisbane Australia Using Vertical Drains and Vacuum Assisted Preloading. In Sound Geotechnical Research to Practice. 539–549.
11. Indraratna B, Rujikiatkamjorn C, Kelly R, Buys H (2012) Soft soil foundation improved by vacuum and surcharge loading. Proc Inst Civ Eng Ground Improv 165(2):87–96
12. Indraratna B, Nimbalkar S, Rujikiatkamjorn C (2014) From theory to practice in track geomechanics–Australian perspective for synthetic inclusions. Trans Geotech 1(4):171–187
13. Indraratna B, Salim W, Rujikiatkamjorn C (2011) Advanced rail geotechnology-ballasted track. CRC Press
14. Selig ET, DelloRusso V, Laine KJ (1992) Sources and causes of ballast fouling, Association of American Railroad (AAR), Report No. R-805, Technical Center, Chicago.
15. Indraratna B, Salim W (2003) Deformation and degradation mechanics of recycled ballast stabilised with geosynthetics. Soils Found 43(4):35–46
16. Indraratna B, Salim W, Ionescu D, Christie D (2001) Stress-strain and degradation behaviour of railway ballast under static and dynamic loading, based on large-scale triaxial testing in Proceedings of the 15th International Conference on Soil Mechanics and Geotechnical Engineering, Lisse, Netherlands.
17. Sun QD, Indraratna B, Nimbalkar S (2016) Deformation and degradation mechanisms of railway ballast under high frequency cyclic loading. J Geotech Geoenviron Eng 142(1):04015056
18. Malisetty RS, Indraratna B, Vinod J (2020) Behaviour of ballast under principal stress rotation: multilaminate approach for moving loads. Comput Geotech 125:103655
19. Indraratna B, Nimbalkar S, Rujikiatkamjorn C (2012) Track stabilisation with geosynthetics and geodrains, and performance verification through field monitoring and numerical modelling. Int J Railw Technol 1(1):195–219

20. Indraratna B, Nimbalkar S, Christie D, Rujikiatkamjorn C, Vinod J (2010) Field assessment of the performance of a ballasted rail track with and without geosynthetics. J Geotech Geoenviron Eng 136(7):907–917
21. Nimbalkar S, Indraratna B (2016) Improved performance of ballasted rail track using geosynthetics and rubber shockmat. J Geotech Geoenviron Eng 142(8):04016031
22. Navaratnarajah SK, Indraratna B (2017) Use of rubber mats to improve the deformation and degradation behavior of rail ballast under cyclic loading. J Geotech Geoenviron Eng 143(6):04017015
23. Indraratna B, Ngo NT, Rujikiatkamjorn C, Vinod JS (2012) (2014) Behavior of fresh and fouled railway ballast subjected to direct shear testing: discrete element simulation. Int J Geomech 14(1):34–44
24. Nimbalkar S, Indraratna B, Dash SK, Christie D (2012) Improved performance of railway ballast under impact loads using shock mats. J Geotech Geoenviron Eng 138(3):281–294
25. Jayasuriya C, Indraratna B, Ngo TN (2019) Experimental study to examine the role of under sleeper pads for improved performance of ballast under cyclic loading. Trans Geotech 19:61–73
26. Qi Y, Indraratna B, Heitor A, Vinod JS (2018) Effect of rubber crumbs on the cyclic behavior of steel furnace slag and coal wash mixtures. J Geotech Geoenviron Eng 144(2):04017107
27. Indraratna B, Qi Y, Heitor A (2018) Evaluating the properties of mixtures of steel furnace slag, coal wash, and rubber crumbs used as subballast. J Mater Civ Eng. https://doi.org/10.1061/(ASCE)MT.1943-5533.0002108
28. Indraratna B, Sun Q, Heitor A, Grant J (2018) Performance of rubber tire-confined capping layer under cyclic loading for railroad conditions. J Mater Civ Eng 30(3):06017021
29. Mazzanti P (2017) Toward transportation asset management: what is the role of geotechnical monitoring? J Civ Struct Heal Monit 7(5):645–656
30. Ngamkhanong C, Kaewunruen S, Costa BJA (2018) State-of-the-art review of railway track resilience monitoring. Infrastructures 3(1):3
31. Bowness D, Lock AC, Powrie W, Priest JA, Richards DJ (2007) Monitoring the dynamic displacements of railway track. Proc Inst Mech Eng Part F J Rail Rapid Transit 221(1):13–22
32. Pinto N, Ribeiro CA, Gabriel J, Calçada R (2015) Dynamic monitoring of railway track displacement using an optical system. Proc Inst Mech Eng Part F J Rail Rapid Transit 229(3):280–290
33. Weston P, Roberts C, Yeo G, Stewart E (2015) Perspectives on railway track geometry condition monitoring from in-service railway vehicles. Veh Syst Dyn 53(7):1063–1091
34. Alemi A, Corman F, Lodewijks G (2017) Condition monitoring approaches for the detection of railway wheel defects. Proc Inst Mech Eng Part F J Rail Rapid Transit 231(8):961–981
35. Indraratna B, Rujikiatkamjorn C, Ewers B, Adams M (2010) Class A prediction of the behavior of soft estuarine soil foundation stabilized by short vertical drains beneath a rail track. J Geotechn Geoenviron Eng 136(5):686–696
36. Indraratna B, Rujikiatkamjorn C, Ameratunga J, Boyle P (2011) Performance and prediction of vacuum combined surcharge consolidation at Port of Brisbane. J Geotech Geoenviron Eng 137(11):1009–1018
37. Kelly RB, Pineda JA, Bates L, Suwal LP, Fitzallen A (2017) Site characterisation for the Ballina field testing facility. Géotechnique 67(4):279–300
38. Indraratna B, Ngo T, Ferreira FB, Rujikiatkamjorn C, Tucho A (2021) Large-scale testing facility for heavy haul track. Transportation Geotechnics 28:100517